



# Georgia Institute of Technology

## HyperJackets

### European Hyperloop Week

Final Demonstration Documentation

March 11, 2022

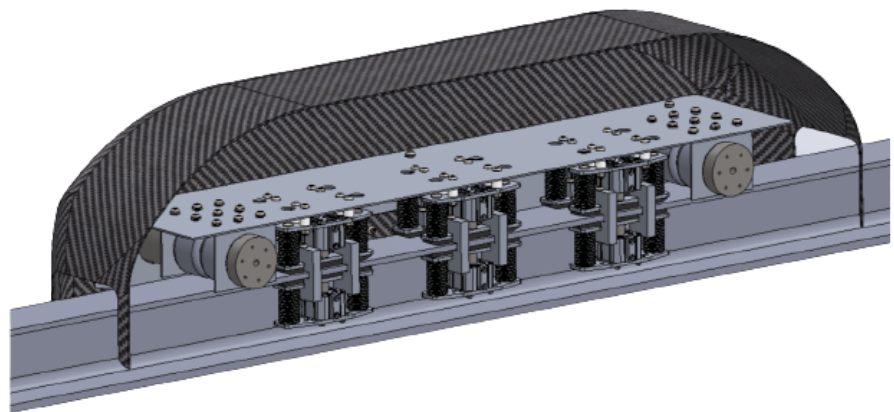


## Table of Contents

<b>HyperJackets 2022 Spring Active Membership Roster:</b>	<b>5</b>
<b>Team Organizational Structure</b>	<b>6</b>
Core Group	6
Aerostructures	6
Electronics	7
Operations	7
Vehicle Dynamics	7
<b>Financing</b>	<b>8</b>
<b>Critical Pod Information</b>	<b>8</b>
Pod Design Overview	8
Mass Table	9
<b>Propulsion</b>	<b>10</b>
Motor Selection & Mounting	10
Motor Testing	10
Wheel Selection	11
Motor Thermal Modeling	12
<b>Stability</b>	<b>12</b>
Theory and Principles	12
Design Process	14
Evidence of Simulations	15
Manufacturing and Integration	16
<b>Braking</b>	<b>17</b>
Theory and Principles	17
Design Process	20
Dimensioning	21
Manufacturing	22
Thermal Analysis	23
<b>Pneumatics</b>	<b>27</b>
Pressure calculations	27
Pneumatic Diagram	27
Design Choices	28
Manufacturing Plans: Pneumatics	28
Testing Plans: Pneumatics	29
<b>Cooling</b>	<b>30</b>
Theory & Considerations	30
Testing	31

Manufacturing and Dimensioning	32
<b>Electronics</b>	<b>33</b>
Energy Storage	33
Manufacturing Plans	34
Battery & Battery Management System	35
Battery & Battery Management System Testing	36
Sensors	37
Sensor Testing	37
Communication	37
Communication Testing	38
Control System	38
Control System Testing	41
General Electronics Testing	42
<b>Aerostructures</b>	<b>42</b>
Aeroshell	42
Chassis	43
<b>FMEA Table</b>	<b>46</b>
<b>Complete Pod Testing Plan</b>	<b>47</b>
<b>Transport and Lifting Plan</b>	<b>47</b>
<b>Acknowledgments</b>	<b>48</b>

**HyperJackets** is a student-led team at the **Georgia Institute of Technology** (henceforth referred to as **Georgia Tech**) that was founded in the fall semester of 2017 and chartered as a registered student organization in 2018. The team currently has members from all six of Georgia Tech's colleges: the Scheller College of Business, the College of Computing, the College of Design, the College of Engineering, the Ivan Allen College of Liberal Arts, and the College of Sciences. We have manufacturing space within the many student-run campus "makerspaces" of Georgia Tech and have access to a full array of machining tools. We also have our own off-campus storage location where we are able to keep our inventory of parts when not in use. As a team and as a campus organization, our goals are threefold:

1. Research, design, build, and test hyperloop pod concepts to improve high-speed ground transportation.
2. Compete in hyperloop competitions.
3. Help Georgia Tech students develop hands-on and theoretical skills to apply to real-word and professional problems.

HyperJackets is divided into four functionally grouped teams: Aerostructures, Electronics, Operations, and Vehicle Dynamics (VD). There is also a process underway to form a research team to compete in EHW's Full-Scale Award research competition. Within HyperJackets, Aerostructures is responsible for the chassis and aeroshell of the pod as well as FEA and CFD modeling. Electronics handles most of the computational coding as well as the electrical hardware. Vehicle Dynamics is responsible for the propulsion, braking, stability, and pneumatics systems, and Aerostructures and Vehicle Dynamics share CAD duties for the pod. Operations handles HyperJackets' business and administrative roles. A research group has also been formed to address the needs of the socioeconomic research competition at EHW, but further steps are needed to make the research group into a "team" at the level described by HyperJackets' bylaws.

With this competition, HyperJackets will endeavor to construct a **complete pod** to run on the track at the 2022 European Hyperloop Week competition in July. The systems and subsystems constituting this year's pod design are outlined in this document.

## HyperJackets 2022 Spring Active Membership Roster:

Name	Role/Team	Name	Role/Team
Charles Malloch	President; VD	Adelya Shakhaidar	Operations
Calvin Dong	Treasurer; Operations	Aditi Tekkam	Research
Jahnvi Hariani	Secretary; VD; Operations	Ariel Watson	Research
Dr. Claudio Di Leo	Faculty Advisor	Allison Williams	Research; VD
Mitul Pandya	Aerostructures	Erik Diehl	Vehicle Dynamics
Zachary Vermeulen	Aerostructures	Trevor Ford	Vehicle Dynamics
Jason Lee	Aerostructures	Catherine Heaton	Vehicle Dynamics
Lloyd Teta	Aerostructures	Mohen Li	Vehicle Dynamics
Junyao Liu	Aerostructures	Liam van den Bogert	VD; Operations
Asante Ndlela	Aerostructures; VD	Shalva Begiashvili	Vehicle Dynamics
Madison Park	Aerostructures	Maggie Caulfield	Vehicle Dynamics
Trevor Stevens	Aerostructures	Lindsey Chiu	Vehicle Dynamics
Isaiah Thompson	Aerostructures	Jacob Epps	Vehicle Dynamics
Frank Yu	Aerostructures	Gabriel Green	Vehicle Dynamics
Rafael Piloto	Electronics	Massimiliano Iaschi	Vehicle Dynamics
Nour Badors	Electronics	Jimmy Li	Vehicle Dynamics
Teddy Feldmann	Electronics	Erica Lull	Vehicle Dynamics
Anthony Hong	Electronics	Sarayu Manikandan	Vehicle Dynamics
Sean Liu	Electronics	Rui Matsubara	Vehicle Dynamics
Giselle McPhilliamy	Electronics	Alexander Nathan	Vehicle Dynamics
Alizeh Premani	Electronics	Clay Schmidt	Vehicle Dynamics
Edward Sun	Electronics	Anisha Singhatwadia	Vehicle Dynamics
Chibodem Udejiofor	Electronics	Yi Tong	Vehicle Dynamics
Manasa Akella	Operations; Electronics; VD	Eric Wen	Vehicle Dynamics
Yuntao Liu	Operations		

# Team Organizational Structure

## Core Group

The Core group has seven members and is composed of HyperJackets' officers; this includes the President, Treasurer, and Secretary, as well as team leads for Aerostructures, Electronics, Operations, and Vehicle Dynamics.. The Core group is responsible for tasks related to organizational structure, administrative duties, systems integration, and maintaining collaboration environments such as the team Slack and Google Drive. Members of the Core group are elected via general body vote at the end of the spring semester to serve 1-year terms beginning at the start of the fall semester. As seen in Figure 1, the President has overall jurisdiction and has 5 members of the Core group directly reporting to them. However, important decisions are made via consensus of the Core group.

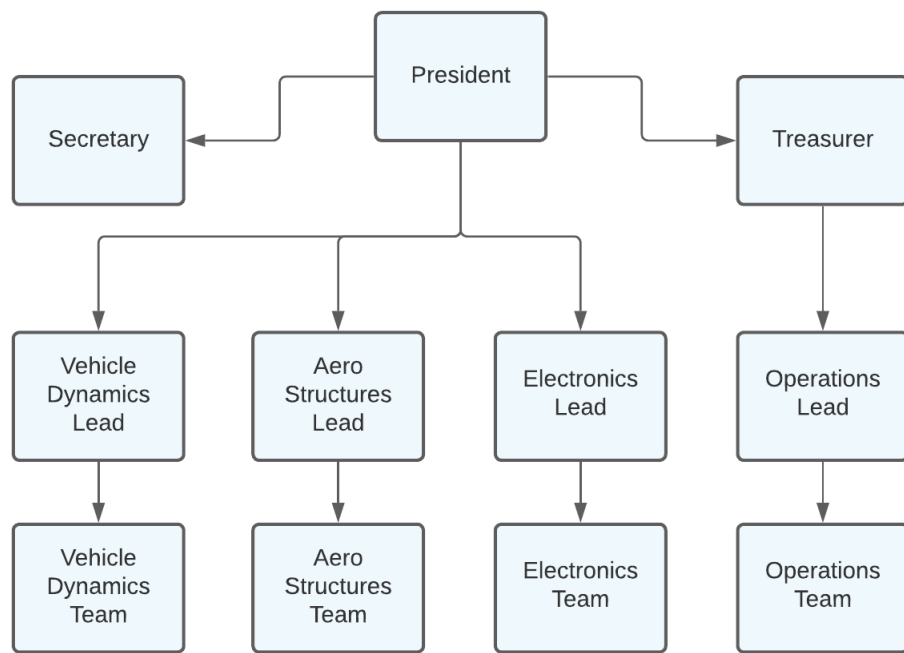


**Figure 1.** Organizational chart showing team structure and chain of command.

## Aerostructures

The Aerostructures team is responsible for the chassis, mounting structures, and aeroshell of the pod. This includes designing mounting points for components, aerodynamic and structural analysis, validating simulations, as well as manufacturing for the aluminum chassis and composites aeroshell. The Aerostructures team is also designing the loading and unloading system and procedures. Aerostructures is divided into two subteams: aeroshell and structures.

Common degree programs for members of the Aerostructures team include aerospace engineering, mechanical engineering, and materials science & engineering.

### Electronics

The Electronics team is responsible for all software, firmware, control hardware and logic on the pod. This includes design, testing, and validation of state machines, PCBs, low/high power battery circuits, motor controllers, PID controllers, and wiring. The team is also responsible for manufacturing any boards and wiring as well as electrical control of the pneumatics system. The Electronics team is divided into two subteams: hardware and software. Common degree programs for members of the Electronics team include computer science, computer engineering, and electrical engineering.

### Operations

The Operations team works closely with the Treasurer to ensure that the team gets sufficient funding to allow the organization to manufacture vehicles and compete in hyperloop pod competitions. As a result, Operations holds jurisdiction over accounting, fundraising, and sponsorship acquisition. Operations also handles administrative duties such as recruiting, campus & community outreach, team merchandise, and website maintenance. Operations is divided into two subteams: administration and finances. Common degree programs for members of the Operations team include business, computational media, and industrial & systems engineering.

### Vehicle Dynamics

The Vehicle Dynamics (VD) team is responsible for all components on the pod that interact with the track or move within the reference frame of the pod at any point during the run. VD is responsible for the design and manufacturing of the pod's propulsive and braking systems. VD also generates any physics models associated with the movement, heating, or stability of the pod. Vehicle Dynamics is divided into five subteams: braking, cooling, pneumatics, propulsion, and stability. Common degree programs for members of the VD team include aerospace engineering, chemical engineering, and mechanical engineering.

## **Financing**

HyperJackets' primary source of funding is through the Georgia Tech Student Government Association (SGA), through a budget given to the club that is approved in the prior fiscal year, as well as bills for funding which are submitted to and approved by SGA during the current fiscal year. SGA funding (budget and bills combined) accounts for approximately \$4800 of our total budget for this year. This type of funding is restricted to requested line items and use cases as defined by SGA. HyperJackets also has an inventory of parts from previous years that is being used for this competition.

The remainder of our budget is from miscellaneous methods of fundraising, such as club dues and fundraising events. This accounts for approximately \$1600 of our total budget.

We are currently in the process of actively seeking sponsors to donate either goods/services or cash. As a registered 501(c)(3) nonprofit organization, we are in an advantageous position for sponsors, as donations toward our organization are tax deductible in the United States.

Procurement is well underway, and most of the materials have been secured for the vehicle's construction. This is bolstered by the use of materials that have been procured in previous years for the SpaceX competitions since those vehicle designs were never fully constructed due to financial limitations. The partial procurement of parts for two previous vehicles has affected the design decisions for this pod in order to HyperJackets' financial needs by incorporating components that are already in the team inventory.

## **Critical Pod Information**

### Pod Design Overview

The goal of HyperJackets with this competition is to design something functional. We do not have ambitions to create the fastest pod or most innovative pod since this is our first time attempting to build a full vehicle. With that in mind, we are sticking with a pod design with critical values as described in Table 1. The pod will have 4 wheels with a direct-drive propulsion

system. The vehicle will have a friction braking system as we have decided that this will be an effective way to stop the pod for a short run distance. The vehicle will be battery-powered, and a battery management system will be used to control power output from our battery pack of 168 batteries. The chassis of the vehicle is 2 parallel plates of waterjet aluminum, and the outer aeroshell will be a carbon fiber composite. We feel that this vehicle design will be a worthy entry into the 2022 European Hyperloop Week Competition, and the details of this design are outlined in the subsequent sections of this document.

**Table 1.** Key pod engineering data.

Critical Figure	Value
Pod length	1.740 meters
Pod width	0.406 meters
Pod height	0.419 meters
Pod mass	81.55 kilograms

## Mass Table

**Table 2.** Mass Measurements of Pod Components.

Item/Component Name and/or Description	Mass, Individual (kg)	Quantity	Mass, Total (kg)	Manufactured in-house, outsourced, or combination?	Section/Subsystem within Pod	Team Responsible	Subteam Responsible (if applicable)
Solenoid Valve	0.207	6	1.242	Outsourced	Pneumatics	Vehicle Dynamics	Pneumatics
Pressure Regulator	0.91	1	0.91	Outsourced	Pneumatics	Vehicle Dynamics	Pneumatics
TP100 Motor	2.93	4	11.72	Outsourced	Propulsion	Vehicle Dynamics	Propulsion
L-Bracket	0.463	4	1.852	In-House	Propulsion	Vehicle Dynamics	Propulsion
Tubing	0.15	1	0.15	Outsourced	Pneumatics	Vehicle Dynamics	Pneumatics
Air tank	2.02	1	2.02	Outsourced	Pneumatics	Vehicle Dynamics	Pneumatics
Wheels	1.48	4	5.92	Outsourced	Wheels	Vehicle Dynamics	Propulsion
Motor axles	0.28	4	1.12	Combination	Wheels	Vehicle Dynamics	Propulsion
Tee Valves	0.057	12	0.684	Outsourced	Pneumatics	Vehicle Dynamics	Pneumatics
Motor axle couplers	0.1	4	0.4	Outsourced	Wheels	Vehicle Dynamics	Propulsion
Air	0.023	1	0.023	N/A	Pneumatics	Vehicle Dynamics	Pneumatics
Stability Springs	0.1307	4	0.5228	Outsourced	Stability	Vehicle Dynamics	Stability
Shock absorbers	0.1982	4	0.7928	Outsourced	Stability	Vehicle Dynamics	Stability
Spring Stability Rods	0.0814	24	1.9536	Combination	Braking	Vehicle Dynamics	Braking
Top Braking Mount	0.126	12	1.512	In-House	Braking	Vehicle Dynamics	Braking
Bottom Braking Mount	0.0986	12	1.1832	In-House	Braking	Vehicle Dynamics	Braking
Linear Actuator Fastener	0.00763	48	0.36624	Outsourced	Braking	Vehicle Dynamics	Braking
Linear Actuator Fastener Nut	0.00388	48	0.18624	Outsourced	Braking	Vehicle Dynamics	Braking
Brake Pad	0.00657	12	0.07884	Combination	Braking	Vehicle Dynamics	Braking
Die Springs	0.191	24	4.584	Outsourced	Braking	Vehicle Dynamics	Braking
Linear Actuator	0.366	12	4.392	Outsourced	Braking	Vehicle Dynamics	Braking
Aeroshell	12.61	1	12.61	In-House	Chassis	Aerostructures	N/A
Top Chassis Plate	4.18	1	4.18	Combination	Chassis	Aerostructures	N/A
Side Chassis Plate	1.68	2	3.36	Combination	Chassis	Aerostructures	N/A
Chassis Corner Machine Bracket	0.0232	6	0.1392	Outsourced	Chassis	Aerostructures	N/A
Chassis Hex Drive Screw	0.021	12	0.252	Outsourced	Chassis	Aerostructures	N/A
Chassis Split Lock Washer	0.0029	12	0.0348	Outsourced	Chassis	Aerostructures	N/A

IMU	0012999957:	1	0012999957:	Outsourced	Electronics	Electronics	N/A
Retroreflective Sensor	0.02012816	2	0.04025632	Outsourced	Electronics	Electronics	N/A
Temperature Sensor	00041515041	10	0041515041	Outsourced	Electronics	Electronics	N/A
Rotary Encoder	0.0005	4	0.002	Outsourced	Propulsion	Electronics	N/A
Motor Encoder	0.0024	4	0.0096	Outsourced	Propulsion	Electronics	N/A
Electronic Speed Controller	0.226	4	0.904	Outsourced	Propulsion	Electronics	N/A
Beagle Bone Black	0.0396893	1	0.0396893	Outsourced	Electronics	Electronics	N/A
CAN Bus	0.048	1	0.048	Outsourced	Electronics	Electronics	N/A
CAN Board	0.003	1	0.003	Outsourced	Electronics	Electronics	N/A
Arduino	0.025	1	0.025	Outsourced	Electronics	Electronics	N/A
Rocket m900 Radio	0.635029	1	0.635029	Outsourced	Electronics	Electronics	N/A
Batteries	0.049	168	8.232	Outsourced	Power	Electronics	N/A
Battery Management System	1.13398	1	1.13398	Outsourced	Power	Electronics	N/A
Approximation of Misc./Wiring Weight	4.53592	1	4.53592	Outsourced	Electronics	Electronics	N/A
Suspension Structure	0.60885	8	4.8708	In-House	Wheels	Vehicle Dynamics	Stability
	Total Mass 81.55144612						

Link to the mass table can be found here: [2022 Pod Mass Table & Parts List](#)

## Propulsion

### Motor Selection & Mounting

We chose to use four 180 KV TP-100 direct-drive motors for the propulsion system of our pod. Their smaller size, theoretical maximum rpm ( $\sim 25,000$  rpm), and high torque (8.78 Nm per motor) allows the propulsion system to be directly driven, reducing the undertaken load per motor and complexity of the system without comprising maximum speed and acceleration. The current estimated pod velocity is about 130.9 m/s, assuming all specifications are close to the manufacturer's claims for each motor. The motors feature six mounting points on the front face, and we have designed a bracket matching the mounting points on the face to fix the motors to. The bracket would then be mounted to the chassis of the pod. The bracket will be manufactured as a blank (no holes) template L-Bracket, which we will then take and bore the correct pattern of mounting features per our design. We have also taken precautions and 3D printed every non-standard component and ensured the robustness and fit of each design.

### Motor Testing

The motor test rig will be constructed to test the maximum rotational velocity of each motor (one at a time) in order to verify the manufacturing specifications, focusing on the maximum speed. The rig will also be used to test battery draw from the motors. The rig itself will be a U-shaped box constructed from 80/20 aluminum t-slotted profiles. On each side of the "U", there will be custom-manufactured L-bracket housing the motor and the encoder respectively. The motor mount features a front-mount for the face of the motor as well as a circular support along the motor to increase stability and attach a small thermal sensor. A coupler

will attach the driving motor (12mm diameter) to a 10mm diameter axle that passes to the other L-Bracket. The receiving bracket has a cutout and cap to fix a bearing for the axle to run through, minimizing friction, as well as a small mounting point for the magnetic encoder. All materials have been acquired for the motor test rig, and testing will proceed in March. The testing will seek to identify the true max rpm of the motors which is expected to be around 25000 rpm as per the manufacturer specifications. Each of the four motors will be tested individually for quality assurance.

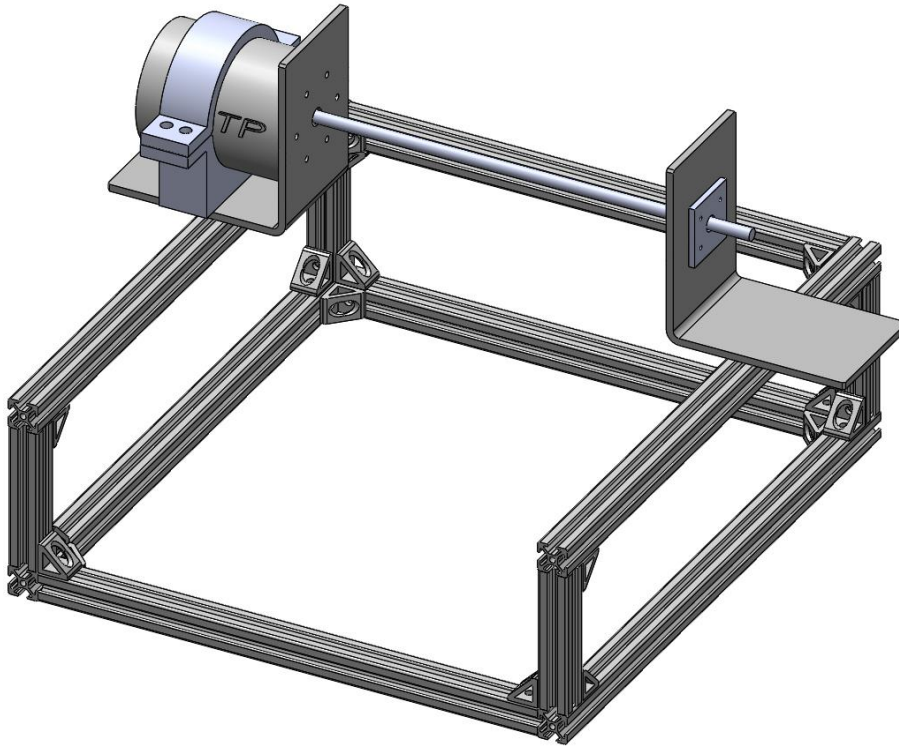


**Figure 2.** Rendered CAD model of testing rig.

### Wheel Selection

We have selected to use a combination of an aluminum core and a polyurethane lining for the wheels. The aluminum core provides a sturdy, yet relatively light, core for the wheels and the thin polyurethane lining helps with maintaining traction as the pod accelerates. The wheel's core will also feature rectangular cutouts around the center axle to help reduce the mass of each wheel. The mass of each wheel is estimated to be 1.5 kg per wheel, using standard 1060 aluminum as the core's material.

## Motor Thermal Modeling

For the motors, transient thermal analysis was performed by applying an internal heat generation load to the motor. This simulation assumes that the motor runs for twice the planned duration of the acceleration phase, and that the motor reaches a peak power twice its rated value. This is far greater strain than would realistically be placed on the motor during the pod's competition runs. The value for heat power generated by the motor assumes a motor inefficiency of 4%, which the manufacturer lists as the worst-case efficiency. In this simulation, the body of the motor reaches a maximum temperature of 37.95 C, which is well within the motor's operating limits.

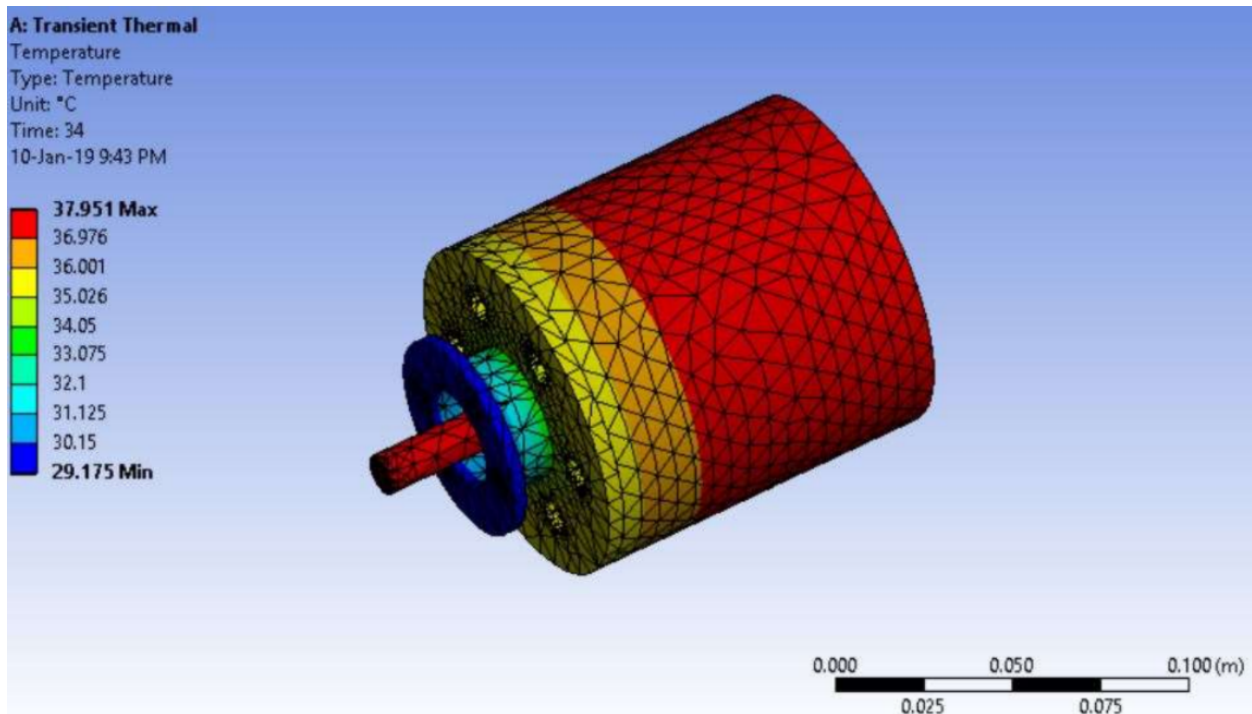


**Figure 3.** Thermal analysis of a TP-100 motor operating at max output conditions. The worst-case scenario has a maximum temperature expected of 37.951 degrees Celsius.

## **Stability**

### Theory and Principles

The stability system is built based on the idea of a Spring-Mass Damper System. A Spring-Mass Damper System is a model composed of discrete mass nodes distributed throughout an object and interconnected through a network of springs and dampers. The model provides us

with the theoretical basis for designing the stability system. It is known that there are two possible circumstances that the pod needs the stability system to overcome the vibration: when the pod faces a bump on the track, and when the pod makes turns. What the pod needs when facing these two conditions is to have forces to support the pod to stabilize the pod onto the track and minimize the vibration of the pod since any huge vibrations could potentially harm the internal structure of the pod, but the potential passengers' experience is also taken into account.

When the pod faces a bump on the track, the pod tends to detach from the track without the vertical stability clamping system due to the conservation of the momentum. It can be simplified into a collision between two objects with an angle. With a short period of suspension in the air, the landing process of the pod would cause severe vibration on the body of the pod. Depending on how large the bump is and the speed of the pod, the pod may also fly entirely off the track in extreme circumstances. Therefore, we designed the vertical stability clamping system that mainly consists of springs and shock absorbers to generate a counter force down onto the track to encounter the potential outcome of facing a bump on the track.

The stability system also includes the horizontal stability clamping system which is designed for the circumstances where the pod makes turns. When making turns on a relatively narrow track, the pod needs a force to balance out the inertia of the pod to change its original motion along the straight line into the new direction. This process needs the generation of a force in the horizontal direction, and due to the uncertainty of the direction of the turns, the horizontal stability clamping system is used on both sides of the pod.

All the units of the stability clamping system work the same as the Spring-Mass Damper System with the springs and the shock absorbers generating the forces needed when facing either bumps or turns on the track.

Using a simple spring-mass-damper differential equation we were able to simulate the movement of the mod where M is the pod mass, C is the damping constant, and K the spring constant. Further detail of the simulation is included below.

**Equation 1:** Spring-mass-damper differential equation

$$M\ddot{x} + C\dot{x} + Kx = Ky + Cy$$

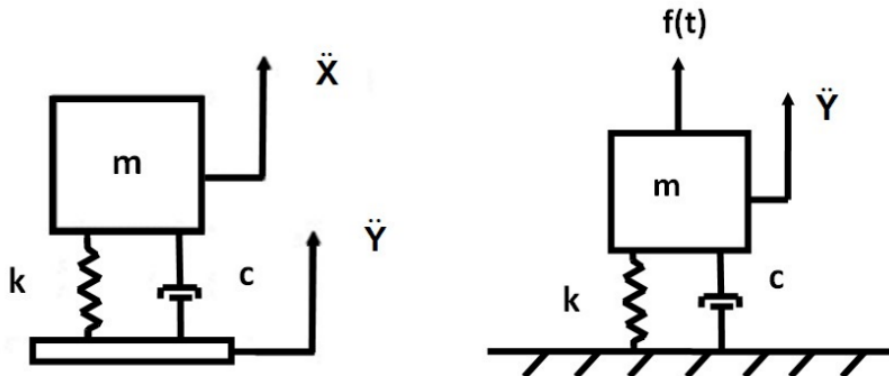


**Figure 4:** Diagram of the DOF system used in the suspension model

Using the spring-mass-damper equations and FBD shown above in our simulations, we chose a spring with spring constant of 19421 N/m.  $Y$  is the position of the wheel relative to zero.

### Design Process

The stability system is modeled off of a simplified train suspension system. Initial suspension research delved into both car and train suspensions and the later was chosen due to a high resemblance to the hyperloop pod concept. High speed trains and freight trains utilize primary and secondary horizontal and vertical stabilizer systems separated by a bogie. The bogie and secondary stabilizer system are typically used for straight and curved tracks and thus only a primary system will be implemented in our pod suspension system. Each wheel will have an accompanying spring damper system that will reduce vibrations from impurities in the track improving the safety of the pod and significantly reduce failure from other systems. The vertical and horizontal suspension designs will be identical. The suspension system will be attached to the main chassis and will consist of a shock absorber inside of a spring mounted to two brackets that are connected to a small wheel that runs beneath the track. This wheel will not be in contact with the prohibited areas of the track. Figure 5 illustrates the design of the system.

The spring shock absorber combination will be attached to the wheel mounting brackets using titanium rods thus the material strength will be greater to reduce connection failures of elements. The brackets were designed to distribute forces safely through the bracket and the pivot on the mounting bracket restricts the movement of the system to one plane.

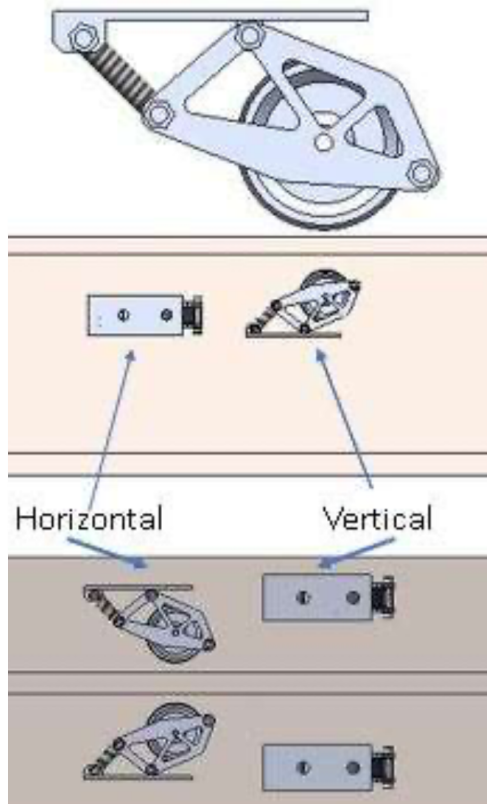


**Figure 5:** Suspension System (Side view, Bottom view)

The wheel will not be providing any thrust or braking to the vehicle and thus the speed will match the speed of the vehicle and there will be negligible heat from the contact to consider.

#### Evidence of Simulations

The following simulation profile describes the horizontal vibrations produced by small irregularities produced by the connection of the track beams. Each track beam was estimated to be 2m long with divots of 3mm.

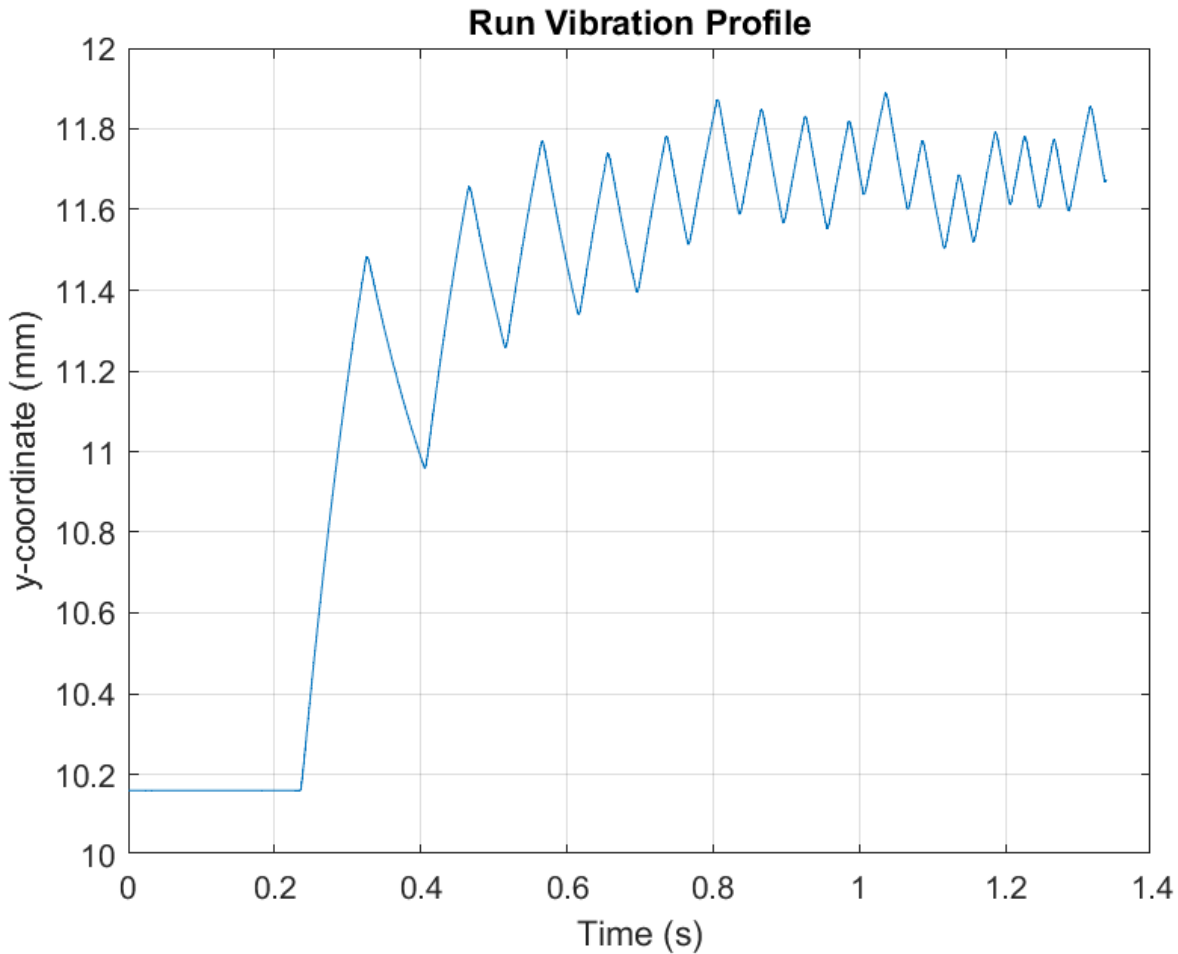


**Figure 6.** Simulation of vertical vibrations from start to target speed.

The figure above shows the response of the vehicle as it traverses 2m intervals along the track length. The simulation accounts for motion within the xy plane and shows a reduction of vibration amplitude with an increase of speed. Additionally the vibrations are minimal and thus ideal for the safety of the pod. These simulation results will be compared to physical hardware tests to ensure their accuracy.

#### Manufacturing and Integration

The spring, shock absorber, and small wheel will be outsourced. The two larger frames and the bracket will be made of aluminum 86 and will be cut out with the OMAX Maxiem 1515 waterjet located in the Georgia Tech Invention Studio. Connections between the elements of the suspension system will be outsourced and cut to size using machinery at Georgia Tech. The

shock absorber spring system will be connected to the mounting bracket and frame using grade 5 titanium rods outsourced from McMaster. This material was selected as these elements will experience high levels of stress and thus must be strong enough to withstand these forces without failure. The spring will be welded onto the shock absorber at the base using equipment at the Georgia Tech Aerospace Machine Shop.

The suspension system will be connected to the main pod using the bracket shown in the CAD model below. These brackets will attach directly to the main chassis frame of the pod. The horizontal and vertical suspension systems will be connected to the main frame separately.

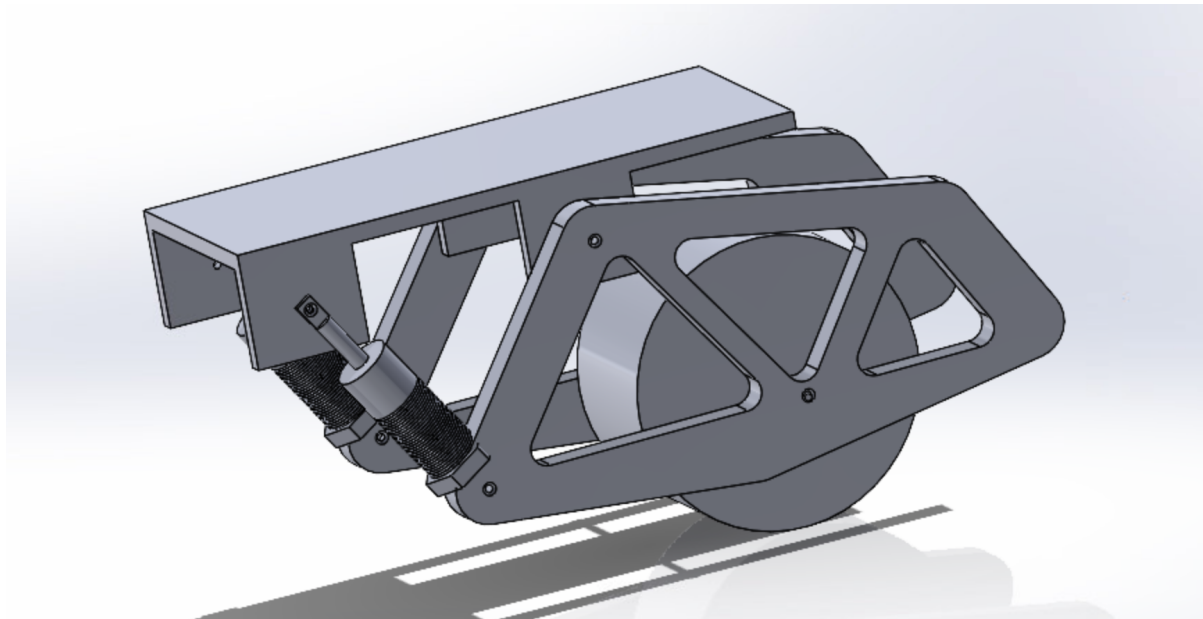


**Figure 7.** Isometric view of individual suspension system. There will be one unit such as the one depicted for each of the vehicle's 4 wheels.

## Braking

### Theory and Principles

The braking system consists of 6 sets of 2 brakes, with each set consisting of one brake on top of the I-beam and one under the I-beam (Figure 8). There are two sets at the front of the pod, two at the middle, and two at the end, with half of the brakes distributed on the left side and the rest on the right side. Each individual braking unit consists of a double acting pneumatic linear actuator (Figure 9-A), die-cast springs (Figure 9-B), stability rods (Figure 9-C), fasteners

(Figure 9-D), mounting plates (Figure 9-E), and a brake pad (Figure 9-F). The forces acting on the pod during braking is shown in Figure 10.

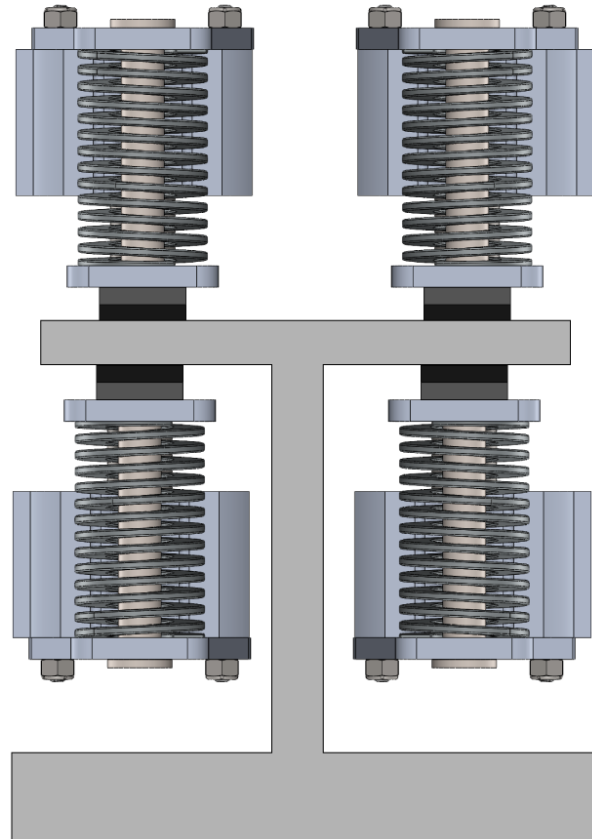


**Figure 8.** Arrangement of brakes on track from front view, not to scale

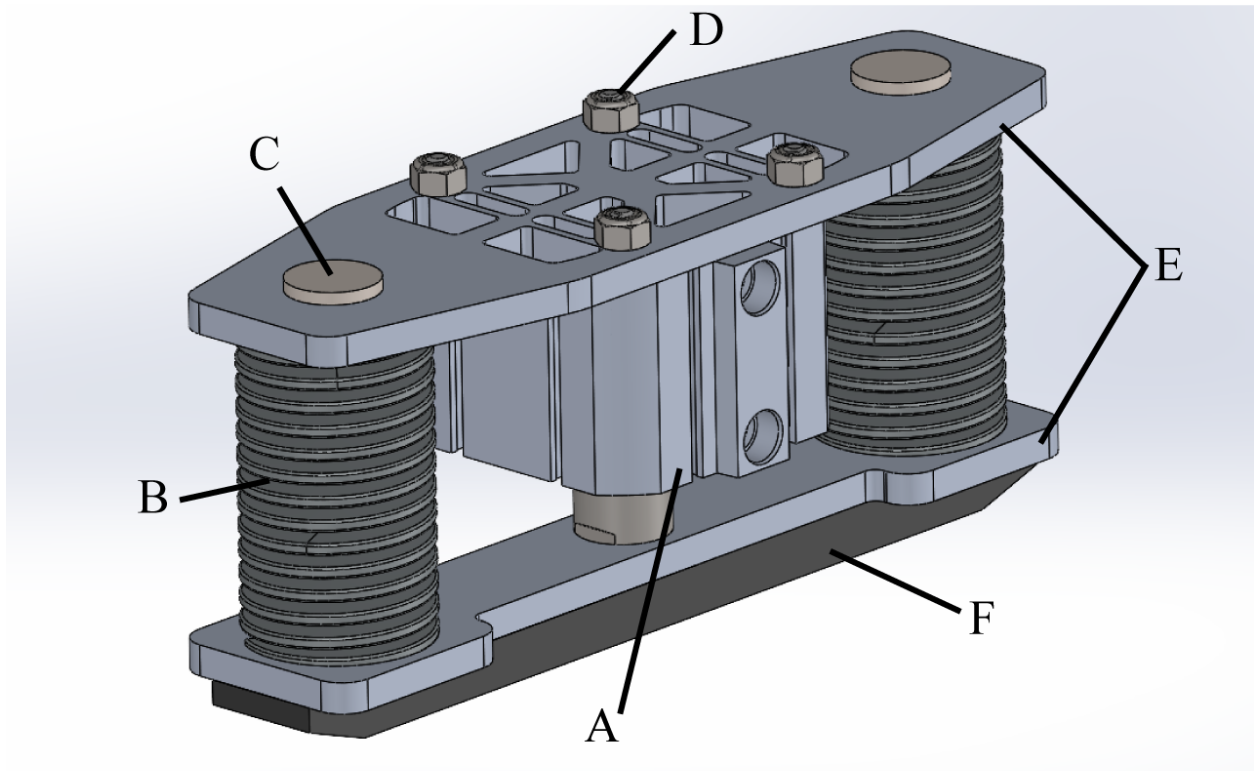


**Figure 9.** Components of a braking unit. There will be 12 such units total.

When the pod is at rest, there is no air in the linear actuators and the brakes are positioned so that the springs are compressed and the brakes are in contact with the track. This ensures the pod will not move when it is at rest. Only when the pod is turned on can air be sent into the linear actuators to raise the brakes off the track. After the pod reaches its maximum velocity, the brakes will be deployed by releasing the air from the linear actuators, allowing the springs to push the brake pad down to the surface of the track. During this process, the stability rods ensure the brake pad and the springs are in alignment. The brakes will gradually deploy over a short period of time so as not to harm the track with a sudden impact. When the braking force reaches a maximum of 6270 N, the pod will slow to a complete stop within 110.5 m. Our braking system also contains an important failsafe; if power is cut from the pod, the linear actuators will release all the air and the brakes automatically begin decelerating the pod. Thus, we do not need to rely on power being supplied to the pneumatic system for braking.

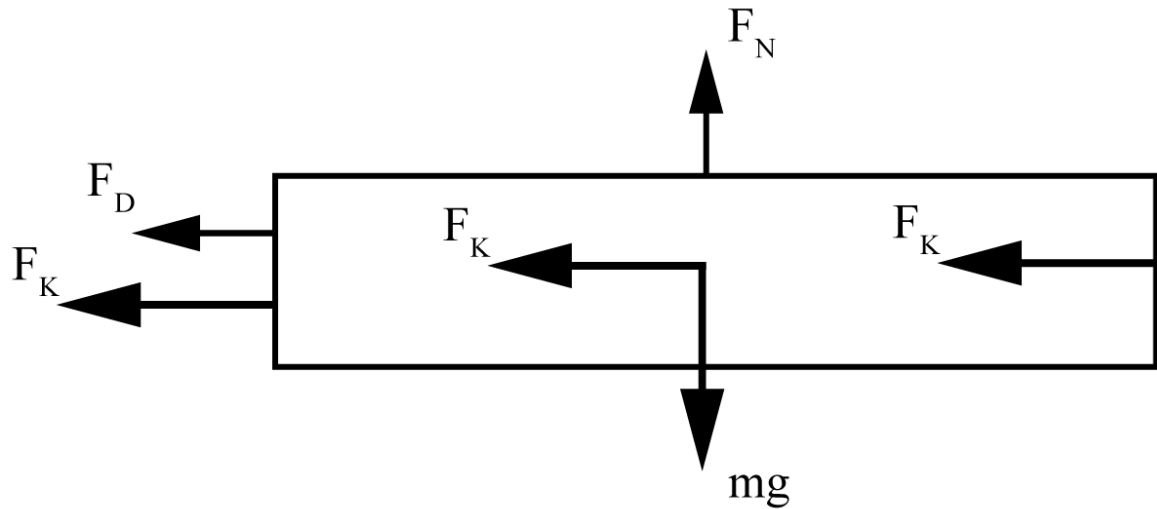


**Figure 10.** Free body diagram of forces acting on the pod while braking.  $Mg$  is weight of pod,  $F_N$  is normal force (from mass and spring force),  $F_K$  is kinetic friction force, and  $F_D$  is aerodynamic drag force. Direction of motion is to the right.

### Design Process

Throughout the entire design process, there were two goals we had: ensure that the brakes would fit into the track's allowable zones on the track and provide the highest possible braking force in doing so. To these ends, we first selected a braking pad material with the highest coefficient of friction and running temperature, which led us to select the RF52 brake material. Then, based on the estimated mass of the pod, we aimed for a braking distance of 110.5 m. Next, we determined that the springs should be compressed 6.35 mm to provide sufficient braking force and have at least 12.7 mm clearance from the track. This led us to choose a linear actuator with 19.05 mm stroke and 50.8 mm bore size. Next, based on our estimated braking distance and

braking force, we choose steel, medium duty springs. If the springs were too stiff, the linear actuators would require too much pressure to release the brakes and the pneumatics system would not be able to generate the required pressure. However, if the springs were not stiff enough, we would not be able to generate the required braking force. Hence, we choose springs with 40 Nm spring rates, which had to be changed to 48 Nm springs, as mentioned previously.

We used steel springs due to steel's high yield strength, which would prevent plastic deformation and strain hardening as the springs undergo high stresses during braking. Similarly, the stability rods are also made of steel to withstand the high shear stresses. We decided to use Aluminum 6061 for the mounting plates to reduce the weight of the braking system and due to its high tensile and compressive strength. As mentioned previously, we choose RF52 material as it can withstand temperatures up to 343°C and has a braking coefficient of 0.55. For the linear actuator, we needed a double-acting cylinder since the brake pad needs to move in two directions, so we chose a customized version of SMC's NCQ8 linear actuator. We choose the smallest stroke and bore size possible for the linear actuator without losing the sufficient force needed to raise the brakes off the track. For the bore size, we still had to ensure it was large enough so that the pneumatics system could generate a realistic pressure in the pneumatic cylinder to raise the brakes of the track.

### Dimensioning

The height of the braking system was based on the highest spring force that we could achieve. At first, we chose a 76.2 mm long spring which would compress 12.7 mm, leaving a 12.7 mm clearance from the track. However, this led to interference with the track so we had to strike a compromise between a higher braking force and the size of the braking system. After testing multiple spring lengths, we ultimately decided to use a 63.5 mm long spring and reduce the compression distance to 6.35 mm. To compensate for the reduced force from the shorter springs, we choose springs with a slightly higher spring rate, from 40 Nm to 48 Nm. We used 6.35 mm thick aluminum for the top and bottom mounting plates and a 6.35 mm thick brake pad, which gives us sufficient braking material to be used over a lengthy time period and a strong backing to prevent premature failure of the brake pads. When the entire braking assembly is in its compressed state, it measures 8.89 cm from top to bottom and its mass is 1.31 kg. The stability rods are 12.7 mm in diameter, the top support plate is 20.4 cm long, and the bottom

support plate is 20.32 cm long. These dimensions keep the braking system small enough to fit within the allowable area underneath the track. See Figure 11 for the side view of the braking system.

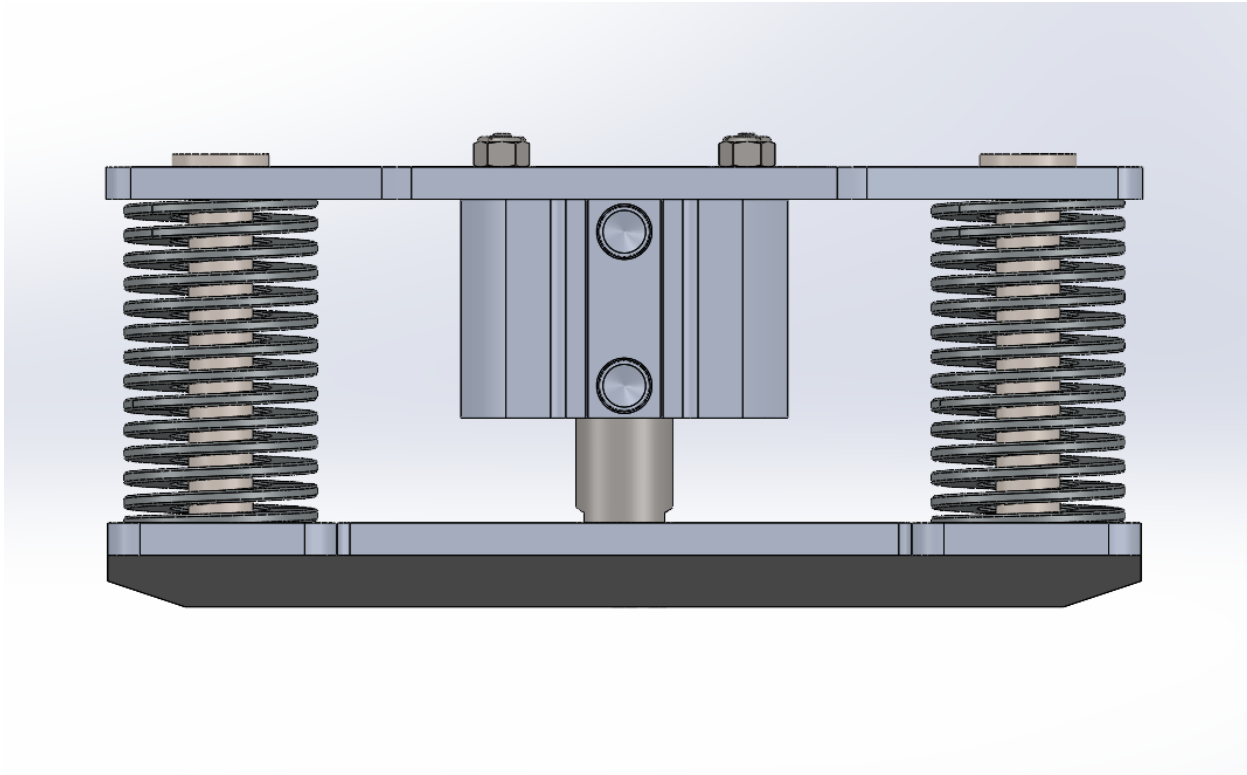


**Figure 11.** Side view of an example of a braking unit, of which there will be 12.

### Manufacturing

To manufacture the braking system, we will outsource the linear actuator, springs, nuts, bolts, and brake pad material. We will waterjet the top and bottom mounting plates out of 6.35 mm thick aluminum sheets and mount the linear actuator to the top mounting plate with four fasteners. Next, we will cut the stability rods out of 12.7 mm diameter steel rods using a cold cut saw or horizontal band saw and weld the bottom of the rods to the bottom mounting plate. The top of the stability rods will be inserted through the springs and respective holes in the top mounting plate and end caps will be welded onto the tops of the stability rods to prevent them from falling out. Meanwhile, the springs will be press-fit into centerbored holes on the top and bottom mounting plates. Finally, the brake pad material will be mounted on the bottom mounting plate via an adhesive similar to what is used in the automotive industry to mount brake pads.

## Structural Analysis

We performed an analysis using ANSYS simulation software on the braking unit while undergoing stress during deceleration. The main areas force was applied were the top and bottom mounting plates where the springs were in contact. The compressive stress in those areas reached as high as 3.81 MPa, which is well under lower than Aluminum 6061's ultimate bearing stress of 607 MPa. Moreover, all the areas being stressed have stresses lower than their respective material's tensile and compressive strengths. Therefore, the structural analysis indicates that the braking system can sufficiently handle the stresses when braking.

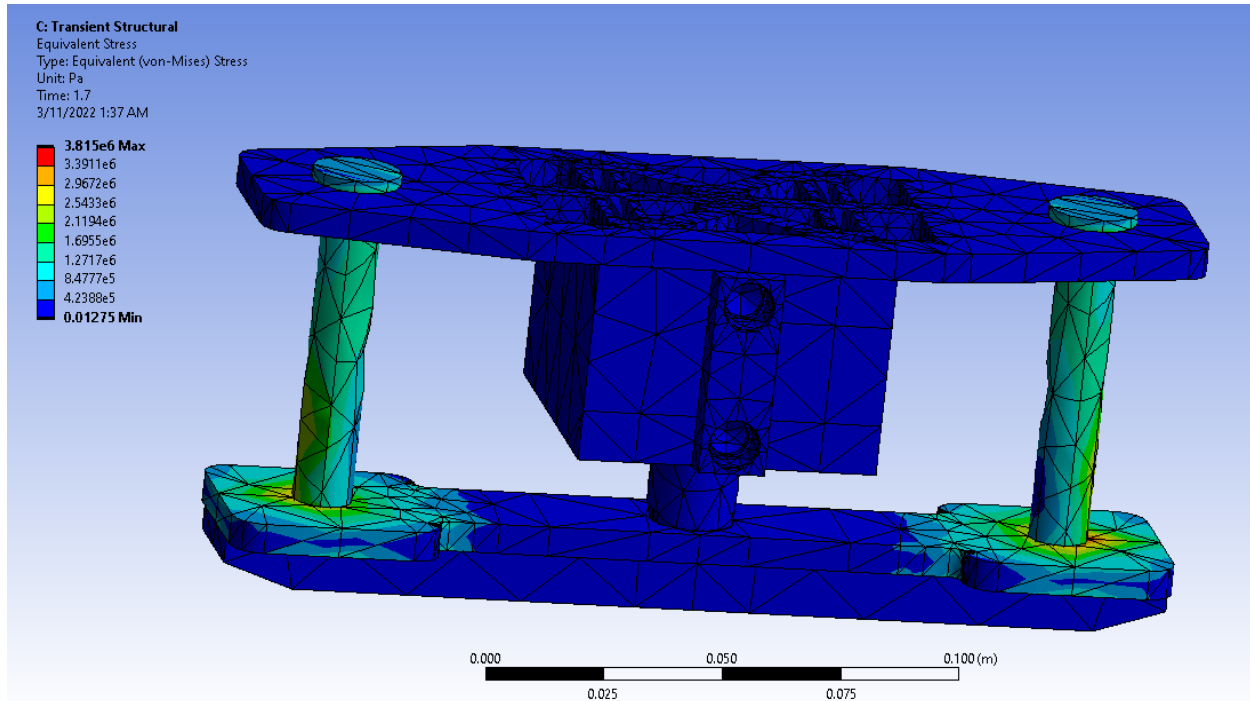


**Figure 12.** Transient structural simulation of brakes undergoing compressive stress during braking.

## Thermal Analysis

Using ANSYS, we determined the maximum temperature immediately after braking was 536.33°C (Figure 1), which is higher than what our braking material is rated for. However, this is only on the outer surface of the brake pad and the inner surface is well under the 343°C our brake pad is rated for. We expect the brake pad to wear away on the outside as well so the current material will be suitable for at least one run on the track. We plan to test the wear rate and temperature of the brake pad material with real-world experiments and will switch our braking

material if it proves insufficient. Furthermore, if needed, we may increase the braking distance to lower the maximum temperatures generated by braking. Figure 2 shows the temperatures after the brakes have been on the track for 2 minutes (including braking time) and demonstrates the brakes cool down sufficiently after braking. We checked and confirmed our simulations using an analytical method in MATLAB which includes heat flows to the brake and track (Figure 3).

Figure 4 shows our loading conditions on the pod during braking, with the red arrows representing the reaction forces experienced during braking. In summary, further real-world testing will be performed to ensure the reliability of our brakes and we will alter the brake pad material if necessary.

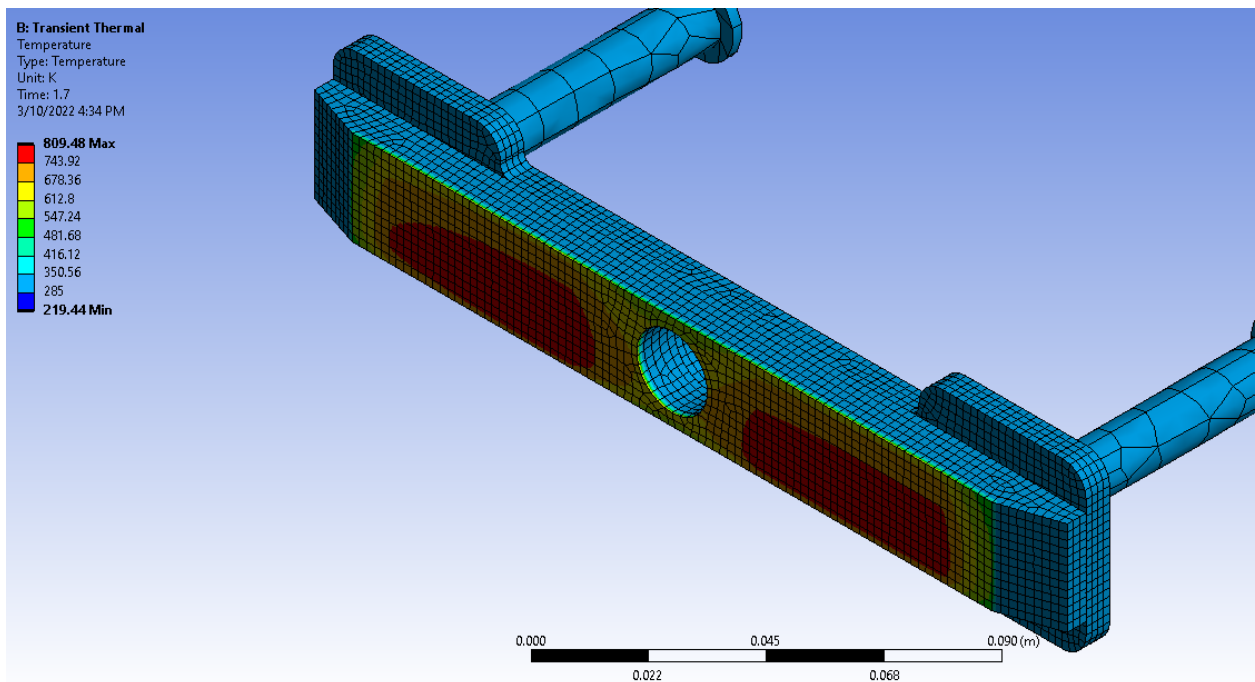


**Figure 13.** Transient thermal simulation of brake system immediately after braking

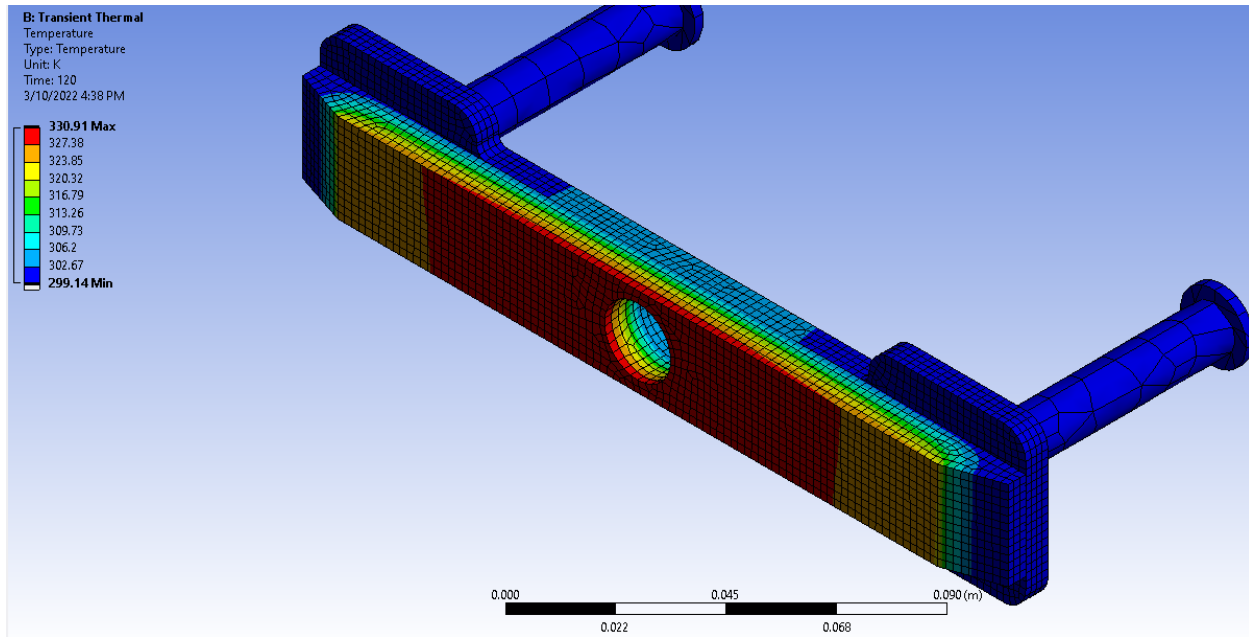


**Figure 14.** Thermal simulation of brake system approximately 2 minutes after braking.

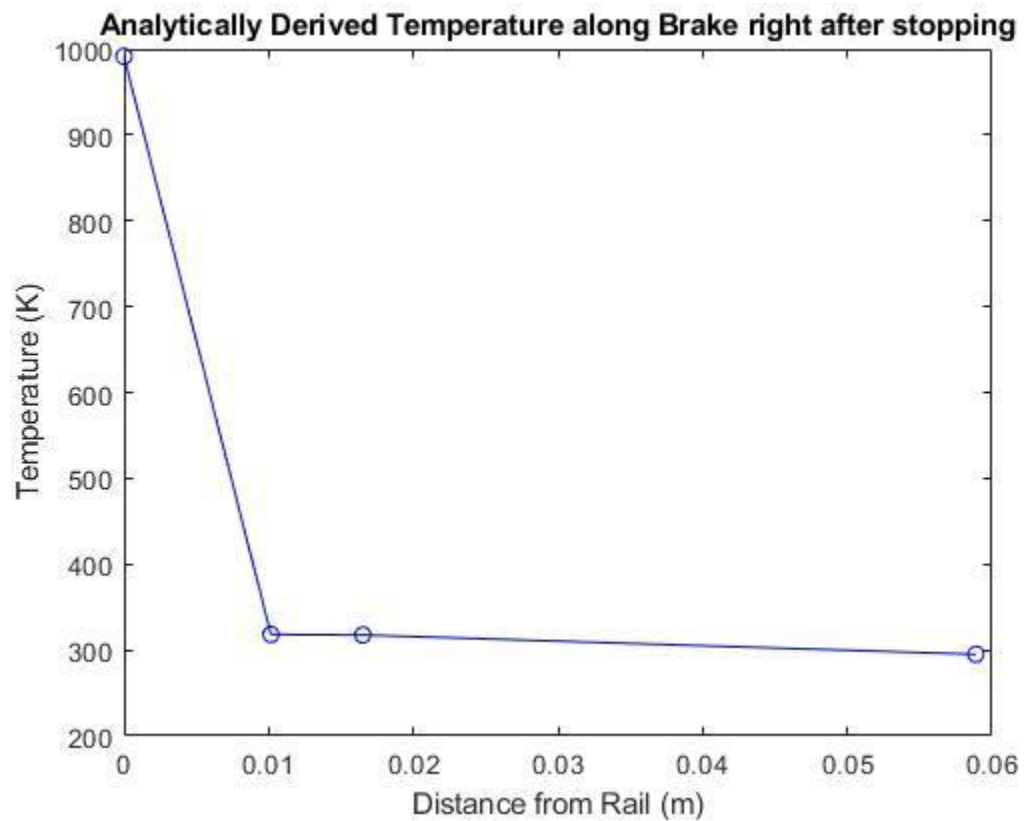


**Figure 15.** Graph of distance from track vs. temperature of braking system immediately after braking

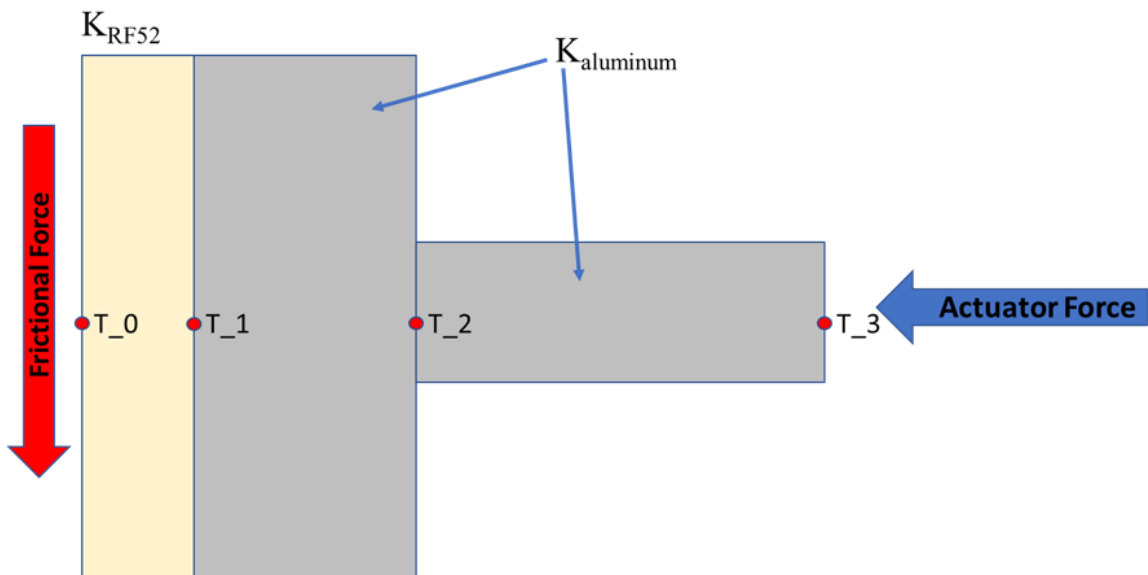


**Figure 16.** Load case for simulation with forces and materials identified. RF52 is the brake pad material.

### Testing Timeline

Our top priority for testing is the reliability of the brake pad material, which includes variables such as the wear rate, running temperatures, and coefficient of friction. We will construct a test rig to test for these variables during April, which consists of our braking material mounted on a fixed, spinning disk. There will be two blocks of aluminum pushed into the sides of the disk with the same linear actuators used in the pod. The actuator will simulate the forces the springs will exert on the brakes during an actual run on the track. The spinning disk simulates the velocity of the pod on the track and the aluminum blocks simulate the track itself. Finally, after we build the braking system, we will test the failsafe mechanism of the braking system and ensure the brakes will activate if the power to the pod is cut. To do so, we will mount one braking unit at a similar position as the real pod, relative to the track. Then, we will repeatedly release and engage the brakes on a slab of aluminum 6061 so we can test the reliability of the brakes and gain a rough idea of the stresses the brakes exert on the track. The stresses have been diagrammed in Figure 16. We aim to finish testing the individual braking system by the end of April and be able to integrate it into the pod for larger scale tests shortly after.

# Pneumatics

## Pressure calculations

Using the bore area of the pneumatic cylinders and the force needed to remove the brakes from the track, the minimum operating pressure inside each of the 12 pneumatic cylinders will be 0.40 MPa. The maximum operating pressure of the cylinders is 1.38 MPa, so the expected operating pressure during a run is significantly below the maximum. The safety factor of the pneumatic cylinders is well over 3. The pressure inside of the 1.9 L tank will not exceed the listed working pressure of 1.034 MPa, although the before run tank pressure will be finalized once all necessary pneumatic components are shipped to Georgia Tech HyperJackets from external suppliers. The pressure in the tank and output pressure from the pressure regulator will be finalized once specifications regarding total length of pneumatic tubing are confirmed.

## Pneumatic Diagram

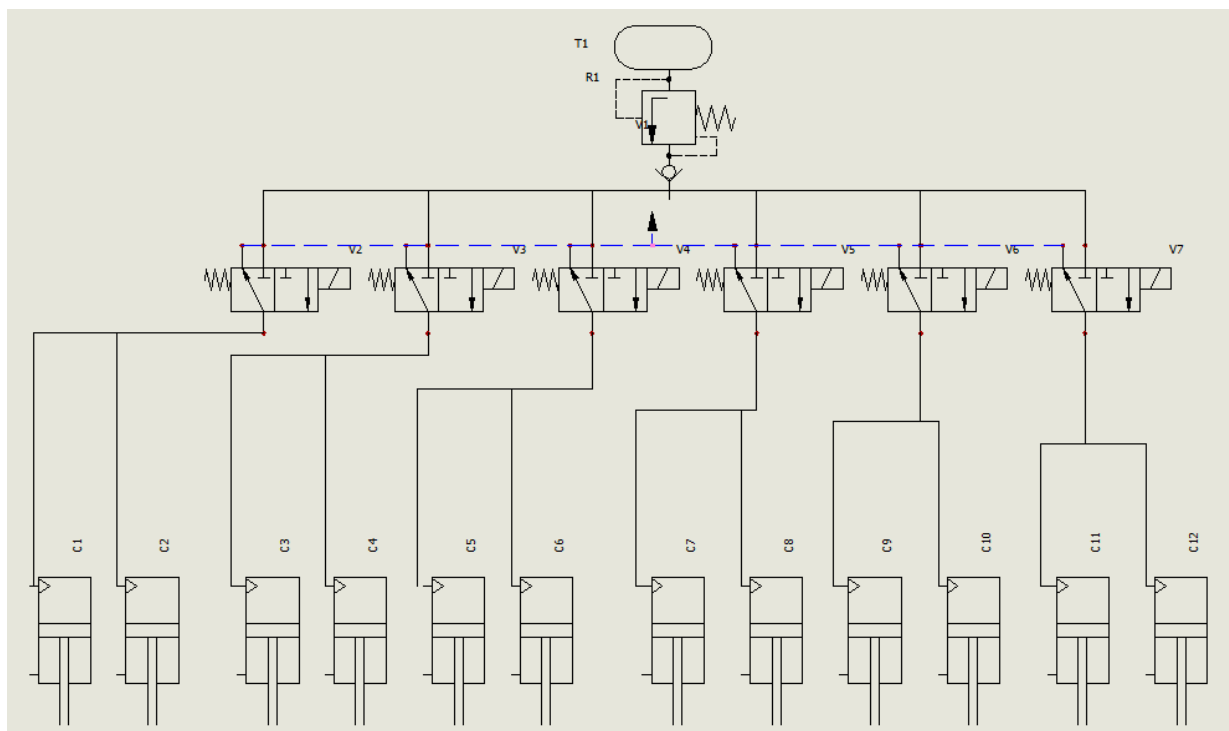


**Figure 17.** Pneumatic diagram showing full architecture of the vehicle's pressurized systems.

Included are 12 pneumatic cylinders to linearly actuate the vehicle's braking system and a pressure regulator feeding air through T-valves and solenoids.

## Design Choices

A 1.9 L steel air tank was chosen due to its compact size and strength. An electronic pressure regulator comes straight from the tank to prevent air from immediately entering the circuit, hence preventing the brakes from removing. The pressure regulator will ensure that air can be stored in the tank and released when activated. Air will be released at a rate and pressure necessary to flow throughout the circuit to each of the 12 pneumatic cylinders. A check valve located immediately after the pressure regulator will act as another fail safe if the regulator fails to stop the flow of air from the tank. A brass tee fitting will connect the check valve to a tube running along the length of the pod. This tube will branch off at 6 locations corresponding to each pair of brakes. Before reaching each pair of brakes (3 top brake pairs and 3 bottom brake pairs) air from the pressure regulator will reach 6 solenoid valves in parallel. Each solenoid valve will correspond to a pair of brakes. When deemed necessary, a current will be applied to the solenoid valves, hence allowing for the flow of air to each pair of pneumatic cylinders. Two position solenoid valves will be used, allowing for either a complete flow or stoppage of air. When no voltage is supplied to the solenoid valves, no air will be allowed to flow to the pneumatic cylinders. However, when 12 V is supplied to the solenoids, the plunger will open allowing for the flow of air. At the final stage in the pneumatic circuit, air will reach one of 12 Air Cylinders with a bore diameter of 1.905 cm and a 1.27 cm stainless steel stroke.

## Manufacturing Plans: Pneumatics

Before building a full pneumatic circuit, individual components such as the air tank, pressure regulator, solenoid valves, and pneumatic cylinders will be tested individually. Once each component is deemed safe and effective, a small scale pneumatic circuit will be manufactured in one of Georgia Tech's student makerspaces, allowing for troubleshooting before a final, full-scale circuit is built. The full scale circuit will likely be manufactured in Georgia Tech's Flowers Invention Studio, an on-campus student-run makerspace. Building a pneumatic circuit is not particularly machine-intensive, so a nylon tubing cutter, valve lubricant, and other basic mechanical tools will be sufficient in the manufacturing process. Among the most important aspects of the circuit is the fit and tightness of the tubing on the brass tee valves. Proper lubrication throughout the valves and tubing will be used to ensure a leak-free design. Another significant factor in the success and safety of the pneumatic circuit is the cleanliness of the air

flowing throughout the circuit. The air regulator attached to the tank will reduce the moisture and buildup of particulate matter.

### Testing Plans: Pneumatics

#### 1.9 L Tank:

The first component of the pneumatic circuit to be tested is the 1.9 L air tank. Without a safe and functioning air tank, every other component of the pneumatic circuit is purposeless. The air tank will be pressurized to max working pressure, 1.034 MPa, to ensure that there are no leaks. The burst pressure of the tank is above 3.447 MPa, but testing procedures will not exceed 1.034 MPa for safety reasons. Before the tank is pressure tested, it will be thoroughly cleaned with soap and water to remove any debris that might've accumulated in storage. Furthermore, the tank will be pressurized to its pre-run pressure to assess consistencies between theoretical mass calculations and actual mass. When fully pressurized, the tank has a mass of 2.02 kg.

#### Pressure Regulator:

To test the pressure regulator, the tank will be pressurized to operating pressure and connected to the regulator. A seamless connection to the tank will be prioritized using necessary lubrication. Then, an electrical input will be supplied to the regulator, and proportional pressure output will be measured using an attached pressure gauge.

#### Solenoid Valves:

The pneumatic circuit uses 0.635 cm NPT 3 way 2 position 12V pneumatic electric solenoid valves. The solenoid valves will be connected to a low pressure source and 12V power supply. Since the valves only have two positions, the valves will be tested with and without a 12 V power supply. When no power is supplied, the valves will not open, thus no air should flow through the valve. A pressure gauge will be attached to the other side of the valve to ensure that there is no air flowing through. Meanwhile, when 12V is supplied to the valves, the valves should open allowing for the complete flow of air. Once each solenoid valve is individually tested, the valves will be connected in parallel to ensure that they operate in synchrony.

## Cylinders:

Similar to the solenoid valves, the cylinders must be actuated simultaneously. Using equal lengths of tubing extending from each solenoid valve, each pair of brakes will be tested individually to ensure that equal pressure and thus braking force is obtained in each pair of brakes. Once each cylinder in each pair actuates at the same time, all 6 pairs of pneumatic cylinders will be run in parallel to ensure equal deployment of brakes.

## Cooling

### Theory & Considerations

As it stands, no cooling system has been fully designed for the pod, but there are several that have been considered and may be implemented, pending thermal testing results. The four options for cooling that have been proposed are a liquid-coolant active cooling system, an air-cooled semi-passive system, a passive ablative/insulative system, and an exclusion of cooling system. In Table 3, a trade study is outlined detailing the costs and benefits of each proposed design.

**Table 3.** Qualitative trade study of proposed cooling systems.

Type of System	Positives	Negatives
Active; Liquid-Cooled	<ul style="list-style-type: none"><li>• Would produce the most effective cooling system</li><li>• Would allow targeted cooling of specific components</li></ul>	<ul style="list-style-type: none"><li>• Costliest system to implement</li><li>• Most complex system</li><li>• Would add the most weight to the pod</li><li>• Would occupy the most volume within the pod</li></ul>
Semi-Passive; Air-Cooled	<ul style="list-style-type: none"><li>• Air intake from outside pod removes need for coolant tank</li><li>• Hardly any weight added to pod</li></ul>	<ul style="list-style-type: none"><li>• Not as effective at removing heat from system as liquid cooling</li><li>• Relies on the movement of the pod to increase volumetric flow rate</li><li>• Would occupy pod space for air-flow</li></ul>
Passive; Ablative,	<ul style="list-style-type: none"><li>• Would allow targeted</li></ul>	<ul style="list-style-type: none"><li>• Does not allow for active</li></ul>

Insulative, and Heat Sinks	<ul style="list-style-type: none"> <li>cooling of specific components</li> <li>Easy to implement as-needed within the pod due to customizable geometry</li> </ul>	mitigation of heating
None	<ul style="list-style-type: none"> <li>Reduces weight of pod</li> <li>Allows for more spare volume within the pod's aeroshell</li> </ul>	<ul style="list-style-type: none"> <li>Necessitates intensive validation of heating expectations for every single component within pod</li> <li>Does not allow for active mitigation of heating</li> </ul>

A robust cooling system would be necessary for any commercial application of a hyperloop transportation system, and this is especially true due to the fact that true hyperloop systems would travel through near-vacuum conditions where air may not be expected to pull any heat out of the vehicle. However, for European Hyperloop Week 2022, the short run time of the demonstration and the choice to run outside in ambient, non-vacuum conditions are factors reducing the need for a powerful cooling system. Our current thermal analysis models for the motors and brakes as seen in Figures 13 and 14 respectively indicate that these systems should not operate at temperatures that will endanger the integrity of the pod. The other systems where heating will be closely monitored are the batteries and the motors' electric speed controllers.

### Testing

The current plan is to conduct thermal testing for all components individually as well as a thermal test of all components simultaneously while within the pod during a test run. These tests will be conducted sequentially, and if any test indicates temperatures exceeding the critical operating range for any components within the vicinity of the overheating component, then cooling measures will be added. All thermal tests will include measurements with thermocouples and verification of results in compliance with TSD rules. As specified in section 12.3.4 of the rules, this verification of compliance with the rules will also include temperature time histories of the aforementioned heat-generating components within the pod and video verification of the

atmospheric conditions the tests are conducted in. There are already temperature sensors within the HyperJackets inventory, so thermal testing should begin in March, starting with the motors.

The motors will not be run at absolute maximum conditions, so the expectations are that the measured temperature values along the outer circumference of the motor will be below the 37.95 degrees Celsius indicated in Figure 3. There is not currently any concern that the brakes will rub fast enough to generate sufficient heat to cause melting of the track surface, but this will also be tested prior to the competition. If it is determined that the test track would be damaged, then the speed of the vehicle will be reduced to reduce the rubbing speed of the brakes, reducing the heat generation.

### Manufacturing and Dimensioning

Our current hypothesis is that

will be able to prove that an active cooling system will not be necessary for the short duration of a demonstration run for this competition. If our testing results determine that cooling needs are present, then we will attempt to address these through passive cooling measures and insulation of heat-sensitive components. This will likely involve the inclusion of additional heat sinks around the batteries and electric speed controllers if it is determined via testing that these components will have temperatures exceeding safe operating ranges. The preferred heat sinks would be CNC machined copper or aluminum since those materials are easily sourced, and the CNC machining will allow for the dimensioning of precise, complex geometries to fit within the available room of the pod. Our expectation is that a heat sink may be necessary for the electric speed controllers, and we have left room within the vehicle to allow for the inclusion of a heat sink if needed. However, these have not been specifically dimensioned yet. Graphite foam may also be used if it may be sourced in a cost-efficient manner. HyperJackets does have a section on the annual SGA budget dedicated to cooling that has not been spent yet, so the team has some flexibility when it comes to cooling solutions.

## **Electronics**

### Energy Storage

The only energy storage found on Electronics is the electrochemical energy stored in our 168 Li-Ion high discharge cells. Each of the lithium ion cells have a maximum capacity of 3000mAh at a safe maximum current output of 30 Amps, resulting in a theoretical maximum output of 5292 Watts at 58.8 Volts and 90 Amps or 5292 Joules of Energy.

**Table 4.** Summary of pod energy storage systems.

<b>Energy Storage Location</b>	<b>Energy Stored (J)</b>
Batteries	5292

## Manufacturing Plans

The general architecture design for electronics has not changed since the ITD Submission. The architecture will closely resemble the following:

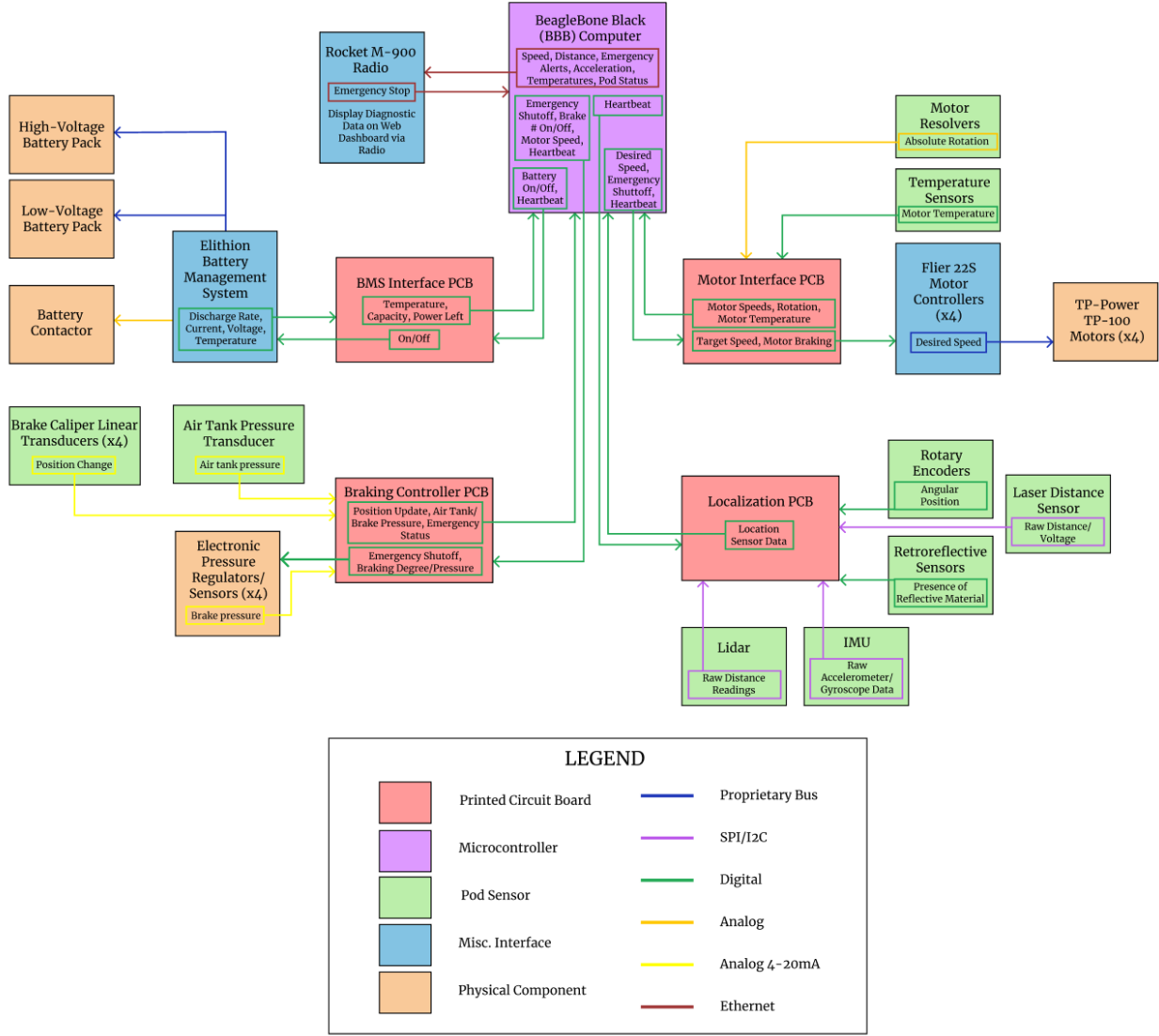


**Figure 18.** Electronics Design Diagram.

Digital signal processing of data collected from the pod sensors will be conducted on the central computer on the pod. Data acquired from the sensors described in the previous section will be transmitted over a Controller Area Network (CAN) bus. The distance readings from the Retroreflective Sensors, Laser Distance Sensor, and Lidar will be combined to determine the total distance remaining on the test track. The acceleration from the Inertial Measurement Unit (IMU) will be used to determine, in conjunction with the distance remaining, how much to accelerate or decelerate the vehicle. The brake pressure combined with deceleration measurements will help determine whether the brakes are working properly, and whether to increase their application pressure. Temperature sensors on the battery management system (BMS) and motors will monitor their status and determine if a component is overheating; if this

occurs, the vehicle may need to be stopped immediately. Currently, the only parts that may be manufactured are the custom printed circuit boards (PCBs) and battery packs. Electronics and parts can be expected to be purchased off-the-shelf and require minor to no modification to integrate into the system.

### Battery & Battery Management System

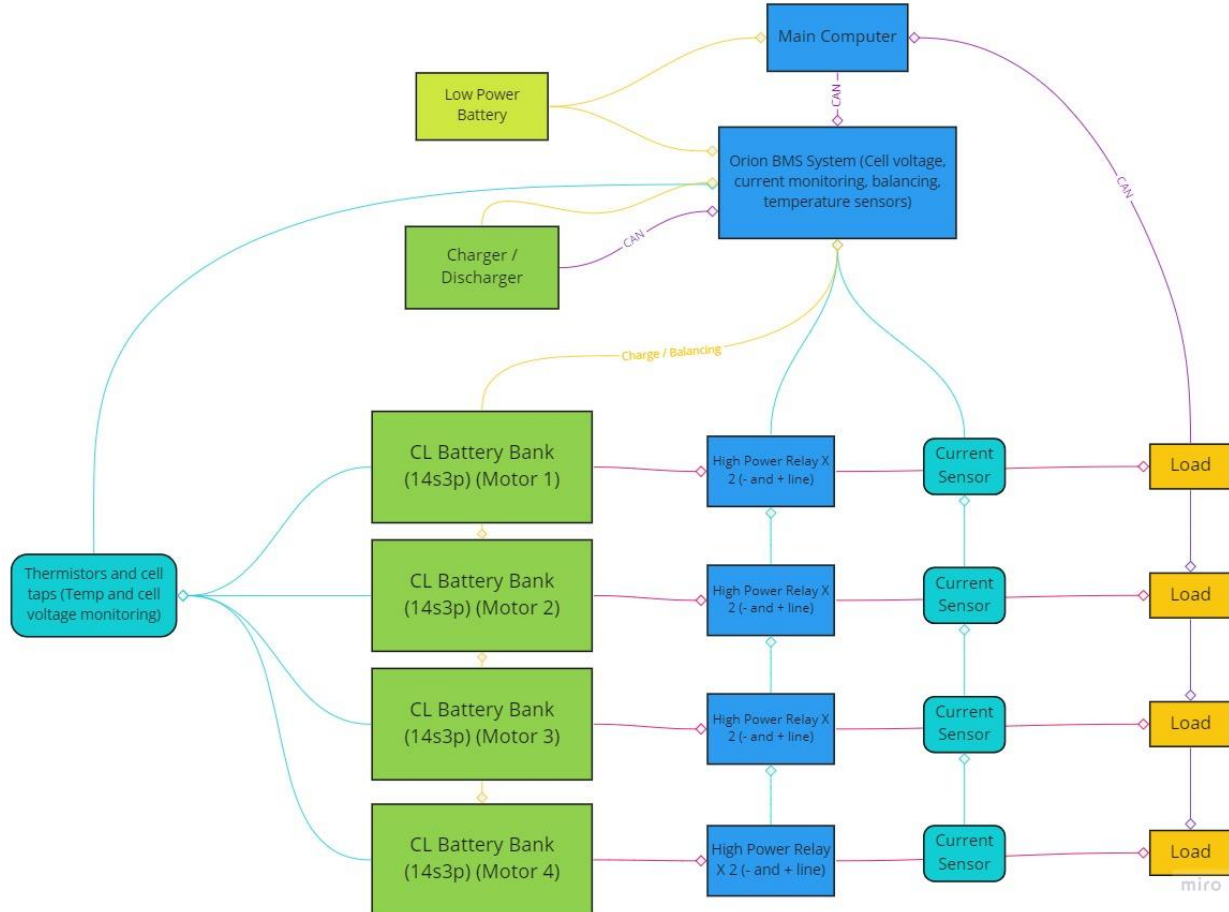


**Figure 19.** Battery and BMS Diagram

In order to nominally drive the 4 TP100 motors using the VESC 6MkV Electronic Speed Controllers, a total of 168 Li-Ion high discharge cells would be required. These cells would be arranged into 4 banks responsible for powering the motors, each containing 42 cells in a 14S3P configuration. Each of the lithium ion cells have a maximum capacity of 3000mAh at a safe maximum current output of 30 Amps, resulting in a theoretical maximum output of 5292 Watts at 58.8 Volts and 90 Amps.

The Orion Battery Management System (BMS) was chosen to regulate the cells for its known reliability in this application and high electrical safety margins. The BMS will be responsible for current monitoring, individual cell voltage balancing, and temperature control for the battery packs.

Various safety systems will be implemented in cases of catastrophic events. This includes: the usage of two normally-open high power relays for each battery pack, the separation between the computational low-voltage and high-voltage electrical systems increasing theoretical control over the high voltage system, and the inclusion of a 120 amp fuse with each bank to prevent overcurrent discharge in case of catastrophic BMS failure.

For communication, the Orion BMS will be connected to the CANBUS to send and receive data to and from the BeagleBone Black's network. Besides the temperature probe lines and cell voltage readout, all other sensor data will be sent over digital lines from the high power system to the BMS.

### Battery & Battery Management System Testing

Testing will occur in multiple main phases:

#### PHASE I A- Basic Validation of Isolated High Voltage Circuit

This phase will validate load circuit functionality. In this phase battery discharge, charge, and capacity will be measured to determine whether the system is within specification for the next phase.

#### PHASE I B - CAN BUS Power on Isolated Computational Low Voltage

This phase validates computational load. In this phase the circuit will have discharge and charge measured while operating only the CAN BUS networks and its corresponding computers. At this point a safety minimum current and voltage can be set for the low voltage computational circuit

#### PHASE II - Low Motor Load Validation on Integrated Circuit

This phase will be computational load in addition to low motor load. The circuit will be run as done in the prior phase except for the exception of the included motors. The motors will be running in their lowest power possible configuration. At this point in testing safety lows for current and voltage can be set for the BMS. Relay functionality will be validated with simulated failures.

## PHASE III - Vehicle Performance Metrics and Thermal Evaluations

The subsequent phases follow the same format as the prior phase in exception to the load from the motor. Phases from this point onward will mainly be for vehicle performance and thermal testing purposes. These tests will occur incrementally up to the circuit's expected maximum operating output. The pod's maximum speed can be determined in the steps providing parameters for brake calibration and cooling system validation.

### Sensors

Currently, we intend to use lidar, IMU, laser distance, rotary encoders, motor resolvers, and temperature sensors to help pod localization and health. Using our microcontroller, the BeagleBone Black (BBB), we intend to read sensor values through CAN. Each individual sensor will provide essential information for our state machine, which will manage the pod based on localization data. The sensors and microcontroller will run on the low voltage circuit.

### Sensor Testing

To accurately test sensor functionality, each sensor will be tested individually for expected conditions in controlled environments. Laser distance sensors will be tested to ensure that distances are accurately recorded at known distances, temperature sensors will be tested to ensure accurate temperature readings at expected and higher temperatures, etc. Then, we will conduct integration testing to ensure that the same results can be observed while transmitting data through the CAN network. This will be an important step in our testing to verify that no one sensor is overloading CAN bandwidth and that no watchdog timers are triggered.

### Communication

During demonstration the team will communicate with the pod through a web dashboard. This dashboard will communicate with the pod through a radio on the wavelengths in the competition instructions. The central computer on the pod will send information about the pod's speed, distance, acceleration, temperature, and emergency status to the dashboard over radio, and the team will be able to send emergency stop instructions to the pod over radio through the dashboard. The dashboard will serve a Google Remote Procedure Call (gRPC) server for cheap and fast data compression/transmission that the pod will connect to. The server will essentially

serve as a TCP server to transmit pod telemetry data which will be displayed on the dashboard. The dashboard will also include an emergency stop button as well as the manual launch button.

### Communication Testing

Pod communication will be tested extensively at various ranges to ensure and verify radio range and bandwidth. Furthermore, unit and integration testing with the gRPC server will ensure that data is properly transmitted and our dashboard will operate the way we expect it to. The HyperJackets will place extra focus on testing the emergency stop communications to ensure reliable and safe performance/behavior.

### Control System

For pod control the HyperJackets will implement a state machine that represents all possible states (unloaded, loaded, safe to approach, ready to launch, launching, breaking, crawling) for the pod defined in our state diagram.

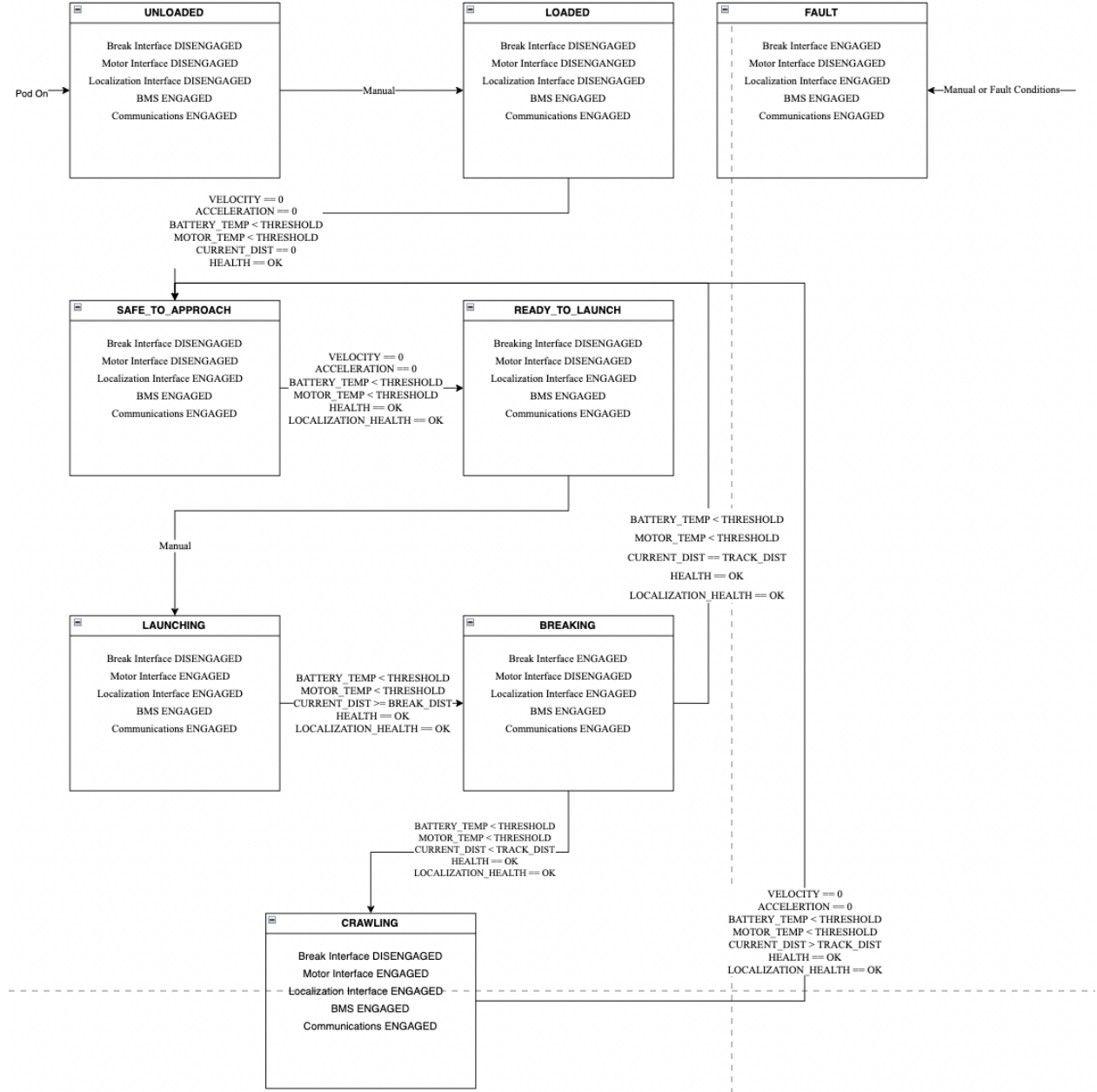


**Figure 20A.** Pod State Diagram.

<b>Variables/Signals</b>	<b>Fault Conditions</b>
BATTERY_TEMP: The maximum temperature of the battery unit as measured by the various temperature sensors	HEALTH != OK
MOTOR_TEMP: The maximum temperature of the motors as measured by the temperature sensors	LOCALIZATION_HEALTH != OK BATTERY_TEMP >= THRESHOLD MOTOR_TEMP >= THRESHOLD
CURRENT_DIST: The pod's relative traveled distance as measured by pod encoders, IMU data, and retroreflective sensors	CURRENT_DIST > EXCEEDED_DIST
HEALTH: The status of overall operating pod sensors. Expected values is close to actual values and manual control communications remains uninterrupted	
LOCALIZATION_HEALTH: The status of localization sensors and agreeing data. (i.e, encoders indicate an expected increase in retroreflective tape)	
TRACK_DIST: The distance at which the pod is expected to come to a full stop	
EXCEEDED_DIST: The distance considered dangerous for continued movement	
BREAK_DIST: The distance calculated to which the pod should begin breaking given VELOCITY and CURRENT_DIST	
THRESHOLD: The threshold considered dangerous for continued movement	

**Figure 20B.** Pod State Diagram descriptions.

Our control system consists of seven main states and the fault state, as seen in Figure 20. Our pod will start in the “UNLOADED” state on power-up. At this point in time, all subsystems will be “DISENGAGED,” meaning not producing any output, except for the battery management system, which will monitor the subsystem’s temperature and outputs as well as communications which will attempt to connect to our dashboard at this time. Once the pod has been positioned and loading has been finalized, the pod will transition to loaded through manual Graphical User Interface (GUI) control using our dashboard. At this time, sensors will be zeroed and monitored for any drifting results. If there is no cause for concern, the pod will transition to

“SAFE\_TO\_APPROACH” where the pod’s localization interface will now engage. In this state, the pod will continue monitoring the zeroed sensors for any drifting observations. If all localization interface sensors indicate a healthy status, the pod will transition to “READY\_TO\_LAUNCH” and then “LAUNCHING” after manual GUI Control. The pod will transition to “BRAKING” once it has reached the calculated “BRAKE\_DIST” and then transition to “CRAWLING” if the pod comes to a complete stop too early. Finally, we transition to “SAFE\_TO\_APPROACH” when we have reached the track distance and we are at a complete stand still. If at any point in time the pod triggers a fault, the pod will transition to a fault state where it will attempt to stop as fast as possible using all methods. Based on various kinematic and temperature data, interface engagement (including braking, motor, localization, BMS, and communications), and health status, the pod will automatically transition between various states to safely traverse the track. The BeagleBone Black, with a clock speed of 1GHz, will step through current data to determine the current state. Based on the current conditions, the pod may observe a “FAULT”, which will safely stop the pod. Otherwise, the pod will transition to the next appropriate step and turn on or off certain interface engagements and change motion profiles.

### Control System Testing

As a crucial part of pod control, we will extensively test the control system through unit and integration tests. With unit tests, we will step, and simulate updating data from sensors and changing the status of GUI controls from the dashboard to simulate pod runs. This will allow us to assert that all interface engagements and pod states are what we expect and that motion profiles are obeyed given the pod state. To ensure that the state machine operates safely, we will extensively test various scenarios such as “perfect” runs and also all scenarios in which the pod should detect a “FAULT”. Last but not least, we will simulate various scenarios outlined in the FMEA to ensure “FAULTs” are detected.

## General Electronics Testing

All electronic components will generally be safely tested through performance and load testing to determine pod limits as well as impact testing to ensure secure wiring and packing of electronic components.

## Aerostructures

### Aeroshell

The aeroshell is 1.74m x 0.406m x 0.419m and serves as the exterior of the hyperloop pod. The manufacturing process will be using a carbon fiber layup. This involves making a female mold that will be machined and then using a carbon fiber and foam, the sheets will be layered until a thickness of 3.175 mm is reached. Using heat guns and orbital sanders, we will smooth out the outside layer and get it to our desired surface finish. Currently, a mock aeroshell is being designed and will allow us to understand this process in better detail.

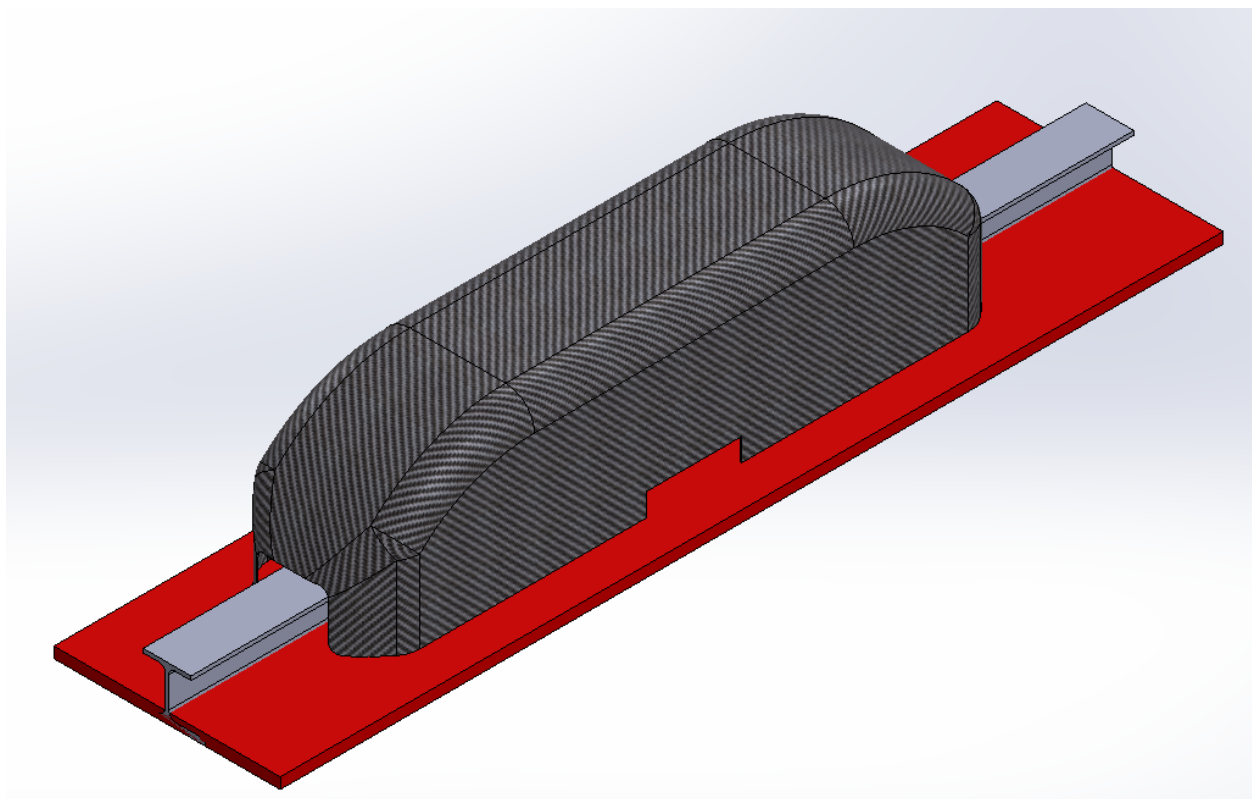


**Figure 21:** Aeroshell Along the Competition Track (red indicating the no-build zone).

## Chassis

The chassis is made of 1/8 inch sheets of aluminum and a waterjet is used to cut out the faces and cut out the necessary holes for mounting onto and around the chassis. After cutting out the faces, we will then join the sheets together to form the shape in the image below. After making this shape, the aeroshell will be joined to the chassis using a horizontal mounting bracket that we will design and a combination of screws and locknut. The chassis of the pod is 55in x 14in x 6in and serves as the backbone that connects all the subsystems together. The goal is to cut the aluminum sheets into the appropriate dimension and also to cut out the necessary holes for mounting other subsystems: electronics, propulsion, pneumatics, stability, and braking. After machining the aluminum sheets, they are joined using L brackets, allowing the sheets to be perpendicular to one another. The specific joining mechanism for each joint (uniform throughout the pod) is a combination of a hex drive screw along with a split lock washer and a locknut. This joining mechanism can be seen in the figure below.

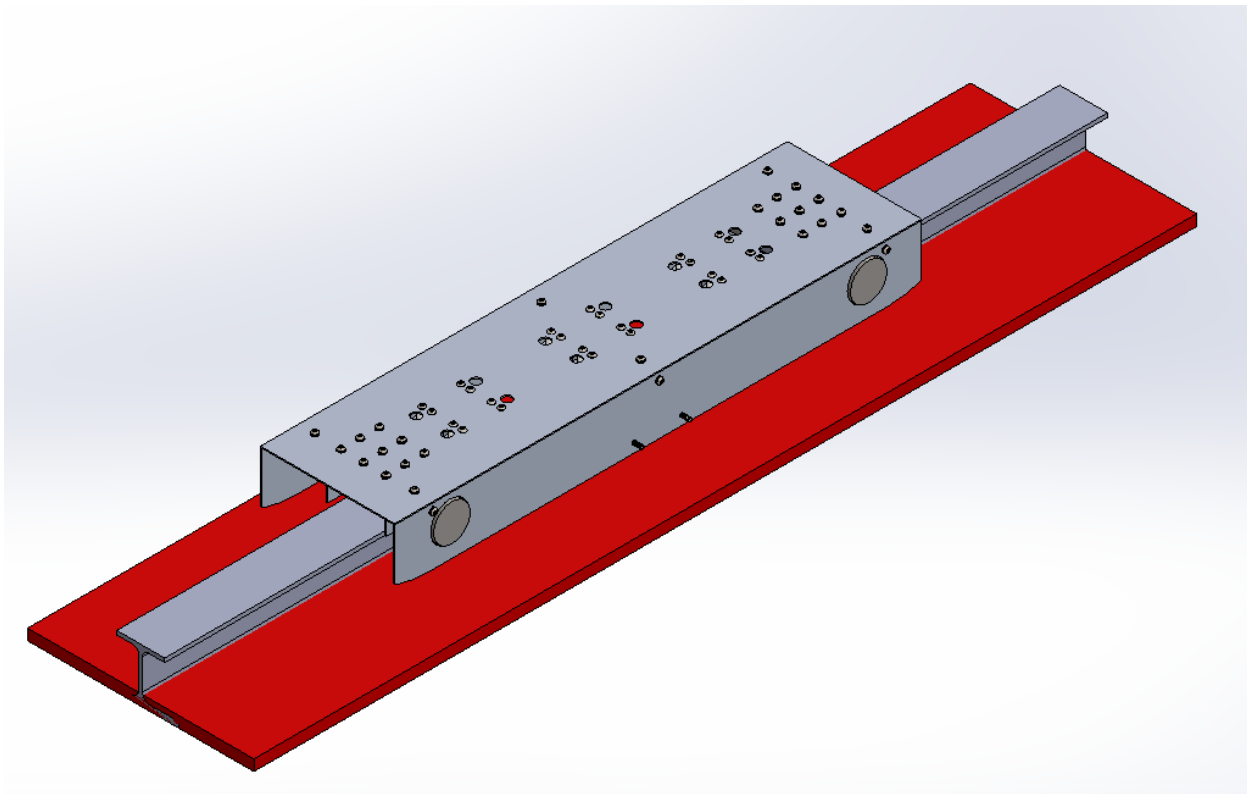


**Figure 22:** Chassis

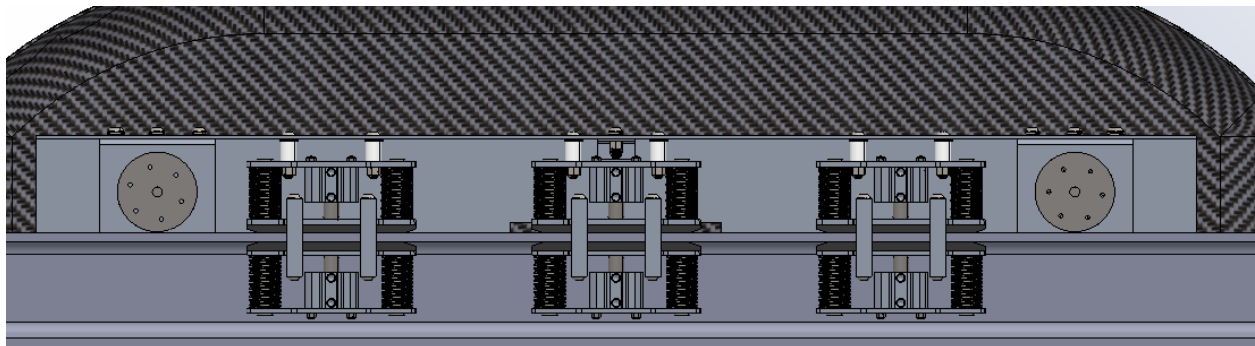


**Figure 23:** Side View of Chassis

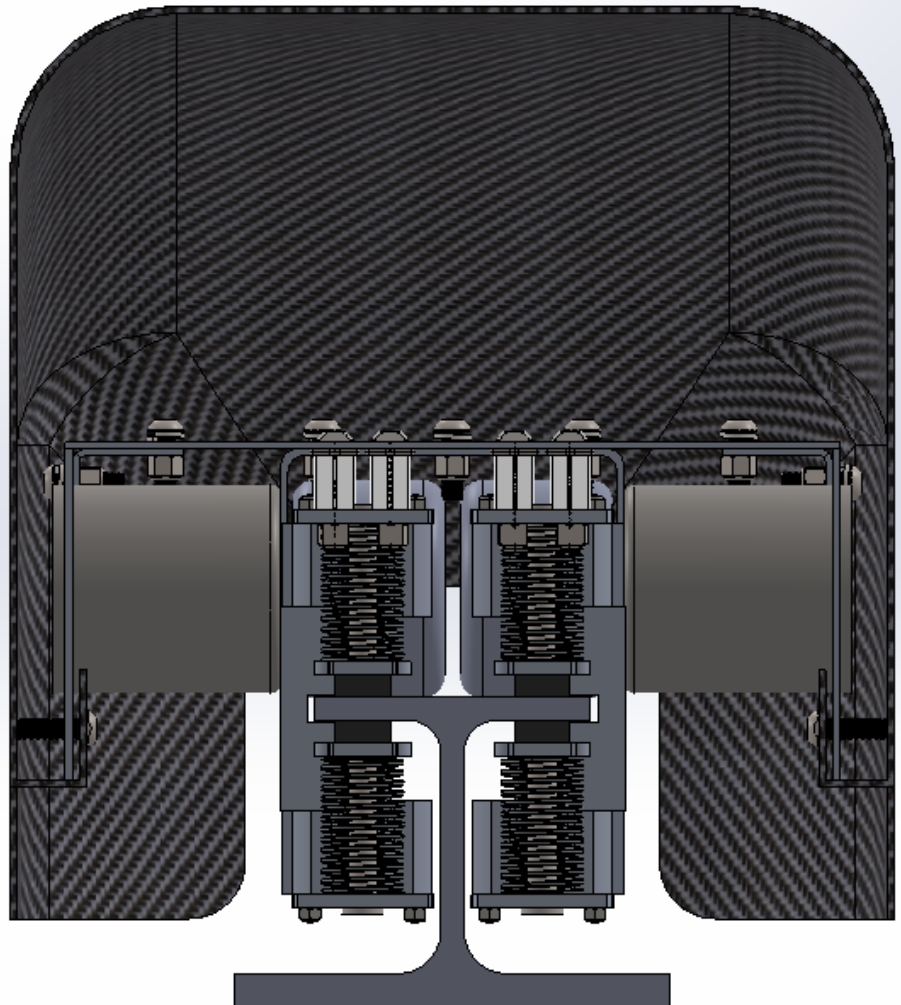


**Figure 24:** Front View of Chassis

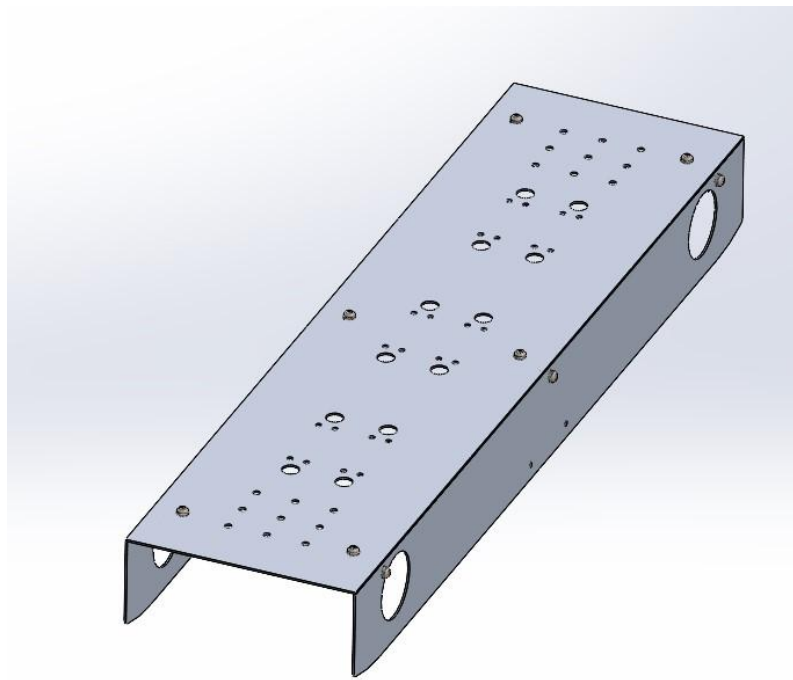


**Figure 25:** Chassis Frame

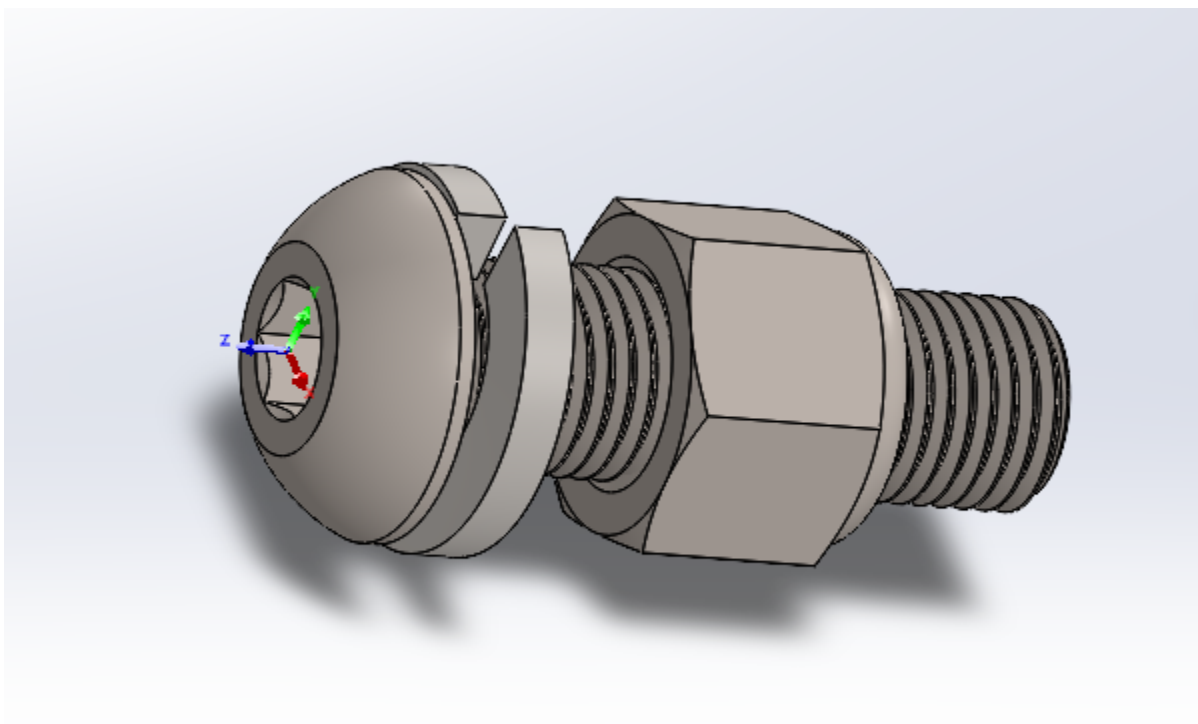


**Figure 26:** Chassis joining mechanism

# FMEA Table

**Table 5.** Failure Mode and Effects Analysis (FMEA) Table

Process Step	Component or System	Team Responsible (Aerostructures, Electronics, Operations, or VD)	Potential Failure Mode	Potential Failure Effects	Probability (1 to 10)	Severity (1 to 10)	Current Controls or Design Measures	Detectability (1 to 10) (1 is the easiest to detect, 10 hardest to detect)	Risk Priority Number	Actions Recommended for Investigation to Solve	Mitigation Requirements
Pod is braking	Brake pad adhesive	VD	High shear forces cause mechanical failure of brake pad adhesive	The brake pad will become detached from the braking mount, and debris in the track could affect the stability of the vehicle	3	9	The braking test rig should address some concerns, and the adhesive was selected with this situation specifically in mind. If properly bonded, it should not be susceptible to failure in shear unless under extreme circumstances.	3	81	Verify in testing that the adhesive functions as advertised in high shear conditions. Manually connect to microcontroller to analyze connection issues	
On pod startup	Microcontroller	Electronics	Failed to connect with dashboard	Cannot communicate telemetry to Dashboard	3	10	Heartbeat control would detect FAULT Passive stability systems have been implemented to dampen out any vibrations from the track. The springs in the braking units will also act as dampeners when impacting.	2	60	Manually connect to microcontroller to analyze connection issues	Reset network manager and reconnect to radio
Pod is braking	Brake pad	VD	Bumps or discontinuities in the track cause large vibrations to transmit into pod while braking	May damage internal pod components and reduce overall vehicle stability	9	3	Validation control detects severe variation from motion profile, FAULT	2	54	Determine via testing the ability of stability systems to dampen vibrations; adjust geometry of brake pad to minimize risk	Shave down leading edge of brake pads to prevent 90-degree angle from impacting bumps or gaps
Monitoring IMU Data	IMU Sensor	Electronics	IMU Drift	Cannot accurately define pod position/heading	2	7		3	42	Monitor IMU Sensor Data when standstill Thermal testing of worst-case braking scenario & a braking test rig to spin an aluminum disc up to maximum expected speeds and press the brake pad material into it.	Reset IMU Sensor, negate drift rate
Pod is braking	Brake pad	VD	Large rubbing speed value creates significant friction and causes the track to become critically hot during a braking run.	The brake pad and track may deform due to excess heating	2	10	The current analytical model suggests the heating will not exceed the melting temperature of aluminum.	2	40		
Pod motors are running	Electric speed controllers	Electronics	Components overheating while in use	Risk of component failure, loss of motor control	4	8	Temperature probes inside pod for entire run	1	32	Rigorous component testing of electric speed controllers at max operating conditions	
On pod startup	Any Sensor	Electronics	Disconnected from microcontroller	Cannot process sensor data	1	10	Heartbeat control would detect FAULT	3	30	Verify port connections	Reconnect & secure sensor
Securing the aeroshell to chassis	Main Horizontal Support	Aerostructures	Part is not properly secured to aeroshell	Aeroshell is unstable, could fall over the pod	3	4	Analysis of fit of aeroshell	2	24	Secure aeroshell using screws	
Wheel separation from axle	Propulsion system	VD	Stress on connecting axle/wheel may lead to warping and damage around the mounting points	Wheel may separate from the pod, possibly derail or damage other systems	2	6	Active monitoring of wear around wheel mounts	2	24	Verify wheel support's structure integrity via testing at max speed conditions	
Triggering solenoid	solenoid valve; tubing	VD	Triggers in a cadence	Brakes are triggered at different times; possible torque generation on pod	3	4	Extensive testing before manufacturing and assembly in pod.	2	24	Test solenoids multiple times to allow time to fix any issues	
Vertical Pod Damping	Vertical Suspension Movement	VD	Suspension wheel contacts the prohibited area of the track	Suspension Failure	1	7	High tolerances and spacings will prevent contact	3	21	Run extensive simulation and physical tests to determine range of movement	
Mounting propulsion system to chassis	Mounting Bracket	VD	propulsion system causing fracture damage to mounting holes due to impulse effects from immediate acceleration	Shearing of motor due to damage, possibly delayed failure if mounting holes unchecked and fractures occur	4	5	Exhaustive testing of bracket and routing checks on mounting points	1	20	Exhaustive testing, possibly adding second bracket or redundancy in case of shearing	
Monitoring battery temp	Batteries	Electronics	overheating	over(discharge/charge)	2	10	Battery Management System measures State of Charge	1	20	Independently measure battery state of charge per cell	Identify & replace bad cells
CAN Communication Monitoring	CAN Board/Bus	Electronics	CAN Communication Disrupted	Pod unable to read sensor data	1	10	Heartbeat control would detect FAULT Monitor internal pod temperature, keep record of tank pressure before run	2	20	Inspect CAN Board wiring & observe telemetry data	Replace CAN Board/Bus
Regulating pressure in air tank	Air tank	VD	Tank overheats and pressure increases	overpressurized, worst case pressure failure leading to rupture	3	6	Extensive testing and simulation running on thermodynamic flow of pod	1	18	Connect a thermometer to the air tank	
Maintaining pod's temperature	Cooling system	VD	Cooling system fails	Pod's motor overheats, can spontaneously combust	4	4	Validation control detects severe variation from motion profile, FAULT	1	16	Rigorous thermal testing of all pod components that generate heat	Add heat sinks where necessary
Pod moving	Motor	Electronics	Motors rotating at different rates	Cannot accurately travel through track	1	8		2	16	Monitor POD odometry while raised	Reset encoder values & use average from both
Mounting propulsion system to chassis	Mounting Bracket	Aerostructures	Stress from propulsion exceeding failure limit	Chassis body separating from propulsion system	3	5	Finite element analysis of bracket	1	15	FEA under max loading conditions; consult with professors to confirm structural safety of the design	
Sending air from tank to pressure regulator	Air hose	VD	Air hose breaches or is not sealed	Brakes are in constant compression; pod does not move	3	2	Extensive testing before manufacturing and assembly in pod.	2	12	See if brake is in compression.	
Triggering solenoid	solenoid valve	VD	Fails to trigger	Brakes are in constant compression; pod does not move	3	2	Extensive testing before manufacturing and assembly in pod.	2	12		

Manufacturing and assembly	Air tank	VD	Air Tank is too heavy	Pod is off balance	2	5	Documenting mass and planning ahead Various Temperature Sensors distributed throughout the pod 3D print the L-bracket first to test if the L-bracket fits onto the motor	1	10	Weigh air tank using a balance to check the mass Identify point of interest through dashboard	
Temperature Sensor Trigger	Temperature Sensor	Electronics	Pod Overheating	Parts could be damaged/on fire	1	10					Colddown point of interest/replace faulty sensor
Stacking the motor onto the L-bracket	Motor Mounting Bracket	VD	Holes position on manufactured piece not perfectly line up with the motor	Motor not fit in to the L-bracket; possible complete failure during operation if forced on	3	1					Test the fit multiple times prior to assembly
State Machine Trigger	Pod State Machine	Electronics	Pod FAULT Triggered	Pod stops and disables	1	5	Pod State Machine validation determined transition to FAULT was successful Sealsants placed around tubing; pressure regulator has 5 um, 0.3 um coalescing and drier filter	1	5	Dashboard telemetry and stack trace in logs	Review stack trace & logs that determined fault
Air flow from tank to cylinder	Pneumatic system	VD	Particle contamination	Blocking pressure, plugged valves; brakes are applied	1	4					Air taken in from different elevation, or remote location Record false positive location and verify there are no retroreflective surfaces
Retroreflective Sensor Trigger	Retroreflective Sensor	Electronics	false positive detection	Incorrectly interprets position	1	2	Current model has enough clearance for larger shocks Examination and quality control	2	4		Clean sensor and remove extraneous retroreflective material
Absorb shock through shock absorber	Shock Absorber	VD	Suspension system encounters larger than expected track irregularity and shock absorber is unable to dampen response	Risk of damage to shock absorber and increased vibrations to the main pod frame	1	4					Investigate IMU data and perform tolerance testing of mechanism Check quality and shape of valves
Air flow from tank to cylinder	Brass T-valves	VD	Deformation	Affects air flow	3	1					Use manifolds to vary air flow to each motor individually
Motor operation	Motor internals	VD	overstressing of motor may lead to burnout/failure of motor to activate (may also be caused by overheating)	lack of power to one or more wheels, may lead to pod instability	3	1	Thermal testing of motors & awareness during operations manufacture small scale prototypes to determine proper amount of lubricant	1	3		Routine filter maintenance, Lubricant testing
Manufacturing and assembly	lubrication of valves and tubing	VD	Too much lubricant=clogged tubing/valves. Not enough lubricant = air leaks or corrosion	Lower than designated pressure sent to break cylinders, brakes may apply	3	1	Temperature probes inside pod for entire run	1	3		Link cooling system to pressure regulator
Regulating pressure from air tank	Pressure regulator	VD	Pressure regulator overheats	Electronics failure	1	2					

Link to the FMEA table can be found here: [+ 2022 EHW FMEA](#)

## Complete Pod Testing Plan

Per the requirements set by DM.3.2, HyperJackets is aware of the need to test the pod on a track prior to the competition in order to receive permission from European Hyperloop Week to run on the competition track. Pending the results of two upcoming fundraisers planned to be held before mid-April, HyperJackets may have the funding necessary to construct a small test track and perform the necessary calculations to extrapolate that data to the full competition distance. If HyperJackets cannot attain this funding in time, the plan is to ask other American-based hyperloop teams for permission to use their test track. Contact has already been made with the leadership of Duke Hyperloop and Gatorloop to pool resources to build a track, and we have also been in contact with the leadership of Texas Guadaloop. Texas Guadaloop has the nearest completed test track to us here at the Georgia Institute of Technology with their track at the University of Texas at Austin. After talking to other organizations, we are optimistic that a test track may be constructed very rapidly once funding is in place.

## Transport and Lifting Plan

To bring the pod from the staging area to the test track a custom-built sled will be used. The sled is made of two parts: the cart and the carrying assembly. The pod sits on a pod-length I-beam resembling the one in the track, with the brakes applied to keep it from moving. This assembly can be moved by 4 people by lifting on the two cross-members at each end. For any

non-walkable distances, the lifting assembly can be rested on top of the cart and will be held in place by four removable pins. Movement of the assembly is restrained by both the wooden panel at the top, and cargo straps that can be routed through holes in the wooden panel. To load the pod onto the track, the cart will be pushed next to the Loading Platform, and the cargo straps will be released. Four team members will lift the pod off the cart and carry it onto the loading platform. Once there, the cross members of the carrying assembly will be unbolted, and the I-beam set on the wooden floor. The pod will be pushed to the alignment rail. Once aligned, the pod will be pressurized, which will release the brakes. It can then be pushed from the carrying I-beam onto the alignment rail. Once there, the top half of the aeroshell will be attached with quarter-turn fasteners. The carrying assembly will be removed from the loading area. To lift the pod from rest on a table to the carrying assembly, 4 custom lifting straps will be manufactured. These will be made of cargo strap, a carabiner hook, and a handle for lifting. The top of the aeroshell will have to be removed and placed on the bottom of the cart. The carabiners will be attached in all 4 corners, by hooking into the slotted aluminum frame.

Similarly to how the pod will be loaded, the unloading process will involve the same customized carrying assembly. The carrying assemblies' I-Beam will be aligned to the end of the track's I-beam. Then the pod will pressurize the brakes, releasing them from the track's I-beam, and the pod will be rolled onto the team's I-beam. Once the pod is completely on the transportation I-beam, the brakes' pressure will be released, locking them. The pod can then be lifted onto the cart to be brought to the exit area or loaded onto a truck with only the carrying assembly, if it needs to be driven. It can be secured with cargo straps there.

Transporting the pod to Europe from the United States will likely involve the use of a cargo vessel, and this is still being worked out. We understand that Duke Hyperloop and Gatorloop have a similar need to determine the most cost-efficient trans-Atlantic transport method, and we will likely attempt to collaborate on this if possible if pooling resources can save us money.

## **Acknowledgments**

Special thanks to Kyle Heiss, John Huang, Nicholas Swaich, Piper Howell, and Daniel Hayes for their instruction and support. Thank you also to the Georgia Tech Aero Maker Space for allowing us to have some extra storage room.